iScience

CellPress
OPEN ACCESS

Article

Hypothalamic and Cell-Specific Transcriptomes Unravel a Dynamic Neuropil Remodeling in Leptin-Induced and Typical Pubertal Transition in Female Mice

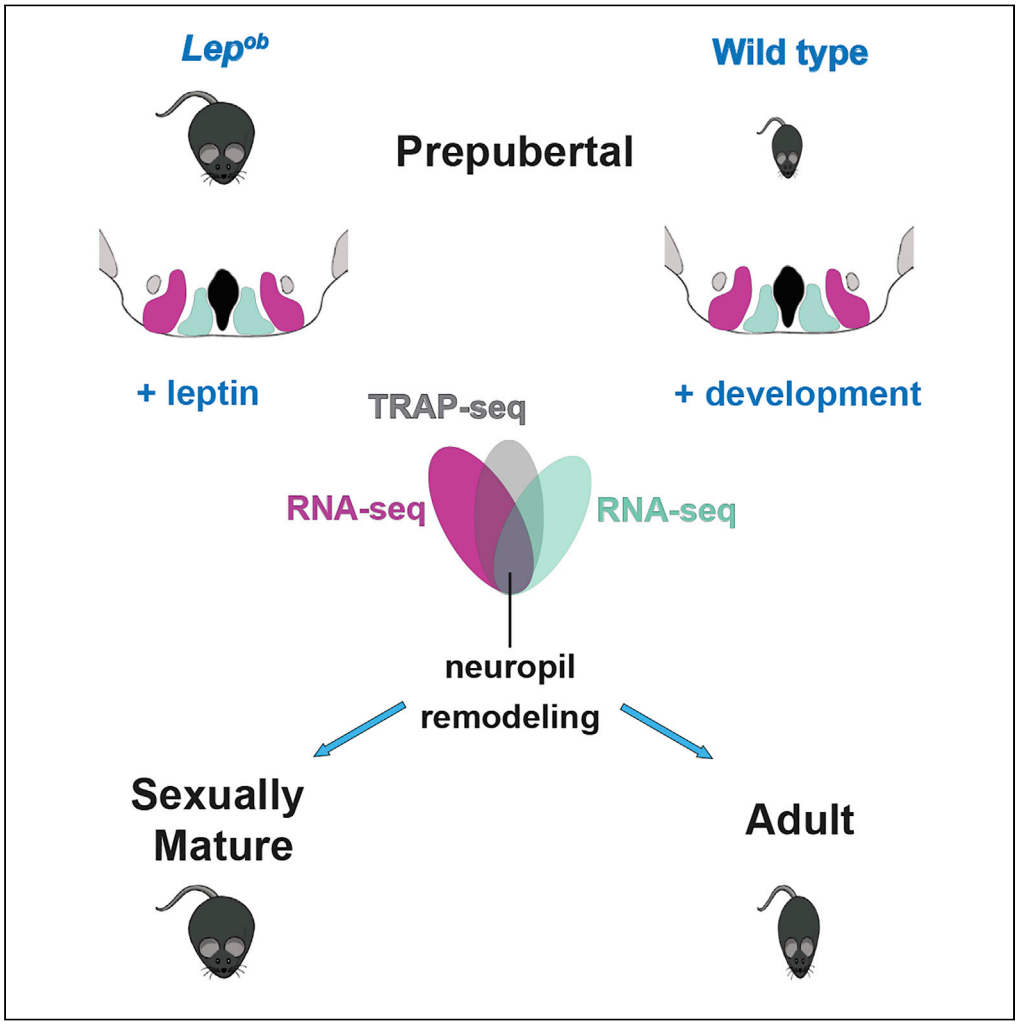

Xingfa Han, Laura L. Burger, David Garcia-Galiano, ..., David P. Olson, Martin G. Myers, Jr., Carol F. Elias

cfelias@umich.edu

HIGHLIGHTS

MBH DEGs between lean and Lep^{ob} mice are highly represented in development

Short-term leptin to Lep^{ob} mice alters MBH DEGs associated with reproduction

PMv/Arc LepRb DEGs between lean and Lep^{ob} mice are abundant in extracellular space

DEGs in developing PMv/Arc are conspicuous in extracellular and neuropil remodeling

Han et al., iScience *23*, 101563
October 23, 2020
https://doi.org/10.1016/j.isci.2020.101563

iScience

CellPress
OPEN ACCESS

Article

Hypothalamic and Cell-Specific Transcriptomes Unravel a Dynamic Neuropil Remodeling in Leptin-Induced and Typical Pubertal Transition in Female Mice

Xingfa Han,[1,2] Laura L. Burger,[1] David Garcia-Galiano,[1] Seokmin Sim,[1] Susan J. Allen,[1] David P. Olson,[1,3] Martin G. Myers, Jr.,[1,4] and Carol F. Elias[1,5,6,*]

SUMMARY

Epidemiological and genome-wide association studies (GWAS) have shown high correlation between childhood obesity and advance in puberty. Early age at menarche is associated with a series of morbidities, including breast cancer, cardiovascular diseases, type 2 diabetes, and obesity. The adipocyte hormone leptin signals the amount of fat stores to the neuroendocrine reproductive axis via direct actions in the brain. Using mouse genetics, we and others have identified the hypothalamic ventral premammillary nucleus (PMv) and the agouti-related protein (AgRP) neurons in the arcuate nucleus (Arc) as primary targets of leptin action in pubertal maturation. However, the molecular mechanisms underlying leptin's effects remain unknown. Here we assessed changes in the PMv and Arc transcriptional program during leptin-stimulated and typical pubertal development using overlapping analysis of bulk RNA sequecing, TRAP sequencing, and the published database. Our findings demonstrate that dynamic somatodendritic remodeling and extracellular space organization underlie leptin-induced and typical pubertal maturation in female mice.

INTRODUCTION

Puberty is an intricate physiological process regarded as the transition from childhood to sexual maturity that develops in a defined period of time (Plant, 2015; Sisk and Foster, 2004; Terasawa and Fernandez, 2001; Wood et al., 2019). It begins with increased activity of the hypothalamic-pituitary-gonadal (HPG) axis induced by stimulation of gonadotropin-releasing hormone (GnRH) neurons (Han et al., 2005; Plant, 2015; Sisk and Foster, 2004). In women, the first menstrual bleeding (menarche) defines the end of pubertal development, the initiation of adult life, and the ability to reproduce. The timing of pubertal development varies among individuals of the same sex, ranging from 8 to 13 years of age in girls and 9 to 14 years in boys. In recent decades, however, increasing occurrence of earlier sexual maturation in girls and, on a small scale also in boys, has been documented (Biro et al., 2006; Herman-Giddens et al., 1997; Kaplowitz et al., 2001; Lee et al., 2010; Walvoord, 2010). These findings have become a matter of intense debate and concern due to the association of earlier ages at puberty with increased prevalence of childhood obesity and adverse consequences in adult life (Ahmed et al., 2009; Biro et al., 2006; Burt Solorzano and McCartney, 2010; Ong et al., 2006; Shalitin and Kiess, 2017; Walvoord, 2010). Premature pubertal development in girls is associated with a series of adult morbidities including breast cancer, cardiovascular diseases, type 2 diabetes, and obesity (Berkey et al., 1999; Cheng et al., 2020; Day et al., 2015, 2017; Lakshman et al., 2008; Petridou et al., 1996; Petry et al., 2018). The molecular mechanisms and the cross talk between metabolism and pubertal development are not fully understood, but tissue- and/or cell-specific genome-wide association studies (GTEx, GWAS projects) have identified the brain as the main site of genetic enrichment of transcripts with roles in age at menarche and/or obesity susceptibility (Day et al., 2017; Locke et al., 2015).

Leptin is a key metabolic cue for sexual maturation and reproductive function. It signals the amount of stored energy in adipocytes to the neuroendocrine reproductive axis (Barash et al., 1996; Chehab et al., 1996; Clement et al., 1998; Donato et al., 2011; Egan et al., 2017; Farooqi et al., 2002). Humans and mice with dysfunctional leptin (*LEP/Lep*) or leptin receptor (*LEPR/Lepr*) genes are obese and fail to enter puberty (Barash et al., 1996; Chehab et al., 1996; Clement et al., 1998; Farooqi et al., 2002). Leptin administration to leptin-deficient subjects restores pubertal development (Barash et al., 1996; Chehab et al., 1996; Farooqi

[1]Department of Molecular & Integrative Physiology, University of Michigan, Ann Arbor, MI 48109, USA

[2]Isotope Research Lab, Sichuan Agricultural University, Ya'an 625014, China

[3]Department of Pediatrics and Communicable Diseases, University of Michigan, Ann Arbor, MI 48109, USA

[4]Department of Internal Medicine, Division of Metabolism, Endocrinology and Diabetes, University of Michigan, Ann Arbor, MI 48109, USA

[5]Department of Gynecology and Obstetrics, University of Michigan, Ann Arbor, MI 48109, USA

[6]Lead Contact

*Correspondence: cfelias@umich.edu

https://doi.org/10.1016/j.isci.2020.101563

et al., 2002). In wild-type juvenile rodents, paradigms of induced high adiposity (small litter size) or increased leptin levels advance puberty (Ahima et al., 1997; Castellano et al., 2011; Kennedy and Mitra, 1963; Yura et al., 2000). The primary effects of leptin are exerted via direct actions in the brain (Cohen et al., 2001; de Luca et al., 2005). Specifically, conditional deletion or re-expression of endogenous *Lepr* gene in mice identified the hypothalamic ventral premammillary nucleus (PMv) and the agouti-related peptide (AgRP) neurons in the arcuate nucleus (Arc) as key targets of leptin action in pubertal development (Donato et al., 2011; Egan et al., 2017; Padilla et al., 2017). However, the molecular mechanisms associated with obesity-induced early puberty remain to be fully elucidated.

In this study, we assessed changes in the transcriptional program of the PMv and Arc in response to leptin in leptin-deficient mice and during typical pubertal maturation in wild-type females. Tissue blocks containing the posterior aspect of the mediobasal hypothalamus, where PMv and Arc neurons are abundant, and micro punches individually targeting each nucleus were harvested. We further assessed the actively transcribed genes in cells directly responsive to leptin (i.e., those expressing the leptin receptor long form or LepRb) during pubertal maturation. Transcripts in LepRb cells were isolated by translating ribosome affinity purification (TRAP) (Allison et al., 2015; Burger et al., 2018). Microdissected hypothalamic tissue and TRAP-isolated transcripts were subjected to RNA sequencing (RNA-seq). Through independent and overlapping analyses of the RNA-seq data, we identified candidate genes in hypothalamic nuclei associated with leptin-induced and typical pubertal development.

RESULTS AND DISCUSSION

Transcriptional Changes in the Posterior Mediobasal Hypothalamus in Response to Exogenous Leptin

To identify genes linking leptin and pubertal development in hypothalamic neurons, we performed transcriptomic analysis of the posterior mediobasal hypothalamus (MBHp) (containing both PMv and Arc neurons, reference images 75–77 in the Allen Mouse Brain Atlas, mouse.brain-map.org/static/atlas) of leptin-deficient *ob/ob* (*Lep*^{ob}) females treated with either saline (named Lep^{ob}) or leptin (named Lep^{ob} + leptin) compared with wild-type mice in diestrus treated with saline (WT), twice daily (n = 4/group). Only normally cycling WT mice were used. After euthanasia, uterine weight was measured to confirm diestrus (<100 mg). After 2 days of leptin treatment (twice daily, total of 2.5 μg/g/day), food intake and body weight of Lep^{ob} + leptin mice were substantially decreased (Figures S1A and S1B) and mice with clear vaginal opening (external sign of puberty onset) were euthanized. One hour after the last leptin or saline injection, a hypothalamic block containing both the PMv and the Arc (MBHp; Figure 1A) was harvested for RNA extraction and RNA-seq analysis. Hierarchical clustering comparing patterns of gene expression showed that Lep^{ob} and Lep^{ob} + leptin mice were closely related (Figure 1B), indicating that short-term leptin treatment, although sufficient for puberty onset, did not restore the full array of leptin-regulated genes.

Pairwise comparison among groups revealed 688 differentially expressed genes (DEGs, Figure 1C; see Transparent Methods for criteria). Of those, 562 DEGs were identified between Lep^{ob} and WT mice (Figure 1C), of which 450 (80%) were upregulated and 112 (20%) were downregulated in Lep^{ob} mice (Figure S1C and Table S1). Well-described leptin-regulated and/or energy balance-associated genes were detected: e.g., *Agrp*, *Npy*, *Pmch*, and *Nr5a1* (*Sf1*) were higher and *Atf3* was reduced in Lep^{ob} mice (Allison et al., 2018; Elias et al., 1999; Elias and Purohit, 2013; Qu et al., 1996; Schwartz et al., 1996, 1998).

To gain mechanistic insights, DEGs were further assembled into gene ontology (GO) subcategories: biological process (BP), cellular component (CC), molecular function (MF), and KEGG pathways (Table S1). Comparing the MBHp of Lep^{ob} and WT, DEGs were annotated into a series of GO terms in all subcategories (Figures S1D and S1E; Table S1). Overall, downregulated DEGs were annotated into neurogenesis and axon development (BP), neuregulin binding (MF), and estrogen signaling pathways (KEGG). Upregulated DEGs were annotated into cell communication, transport, reproductive function, morphogenesis, and growth. They were primarily associated with extracellular compartment (e.g., *Adamts4*, *Abi3bp*, *Col22a1*, *Col5a3*, *Col6a1*, *Col6a2*, *Lamb3*, *Lamc2*, *Anxa1*, *Omd*) and plasma membrane and were involved in transmembrane transport, protein dimerization, receptor binding (e.g., *Ramp3*, *Ccr5*, *Prokr2*, *Adab2*, *Gpr4*, *Mc3r*, *Gpr88*, *Slc6a3*), PI3K pathway (*Pik3c2b*, *Cdkn1a*, *Sgk3*), focal adhesion, extracellular matrix-receptor interaction (*Adamts18*, *Cd46*, *Fgl2*, *Prkcd*, *Tfrc*, *Shh*), and protein processing. A number of these DEGs have been described in GWAS longitudinal studies or rodent transcriptome analyses focused on sexual development and idiopathic hypogonadotropic hypogonadism, e.g., *Prokr2*, *Mc3r*, *Six6*, *Adcy28*,

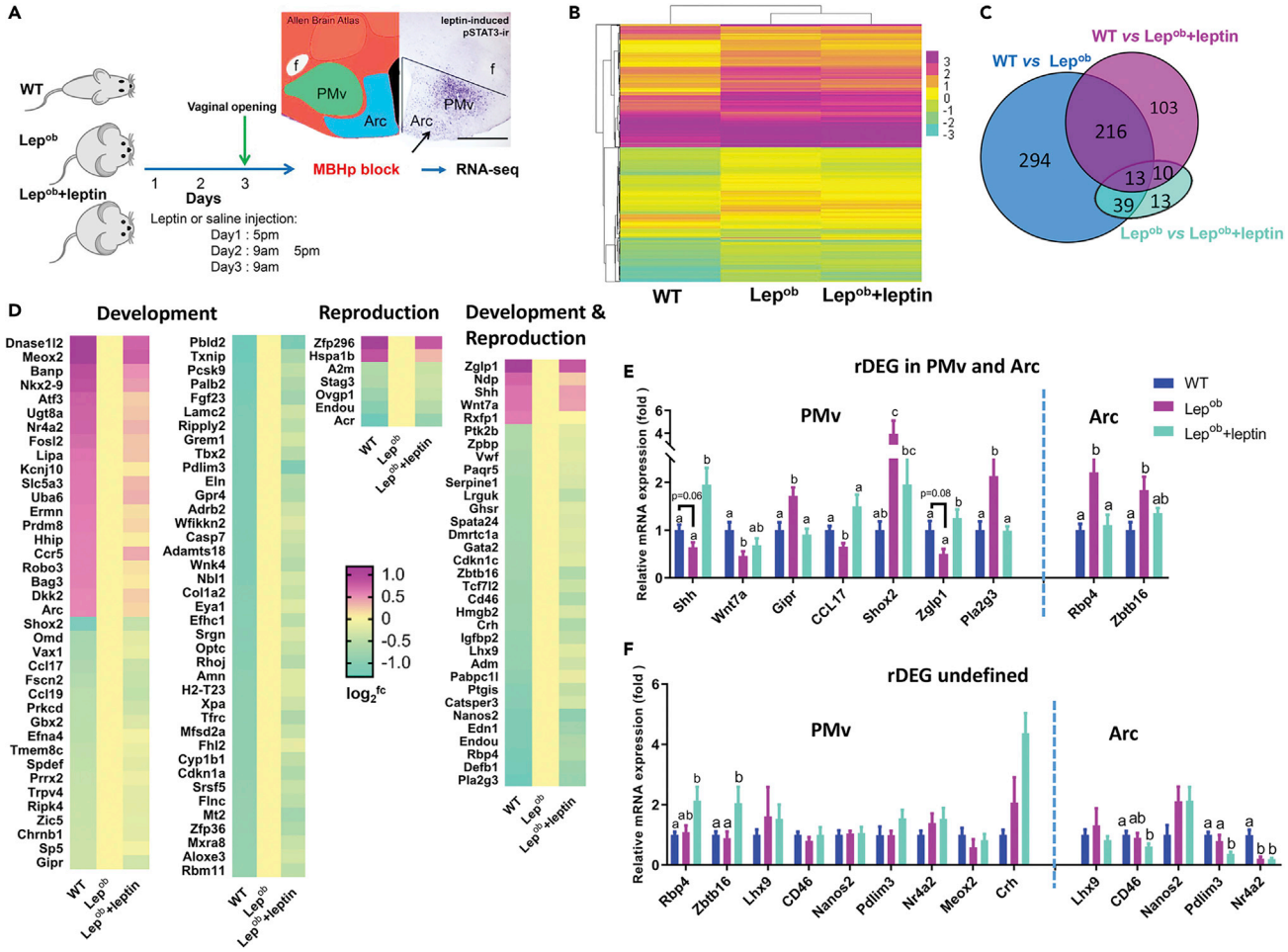

Figure 1. Transcriptional Changes in the Posterior Mediobasal Hypothalamus (MBHp) in Response to Exogenous Leptin

(A) Illustration of experimental groups. Mice were divided into three groups (n = 4/group): wild-type diestrous treated with intraperitoneal (i.p.) saline (WT) and leptin-deficient females treated with i.p. saline (Lep^{ob}) or i.p. leptin (Lep^{ob} + leptin). After 4 injections of leptin, twice daily, puberty onset was observed. Mice were euthanized 1 h after the last saline or leptin injection. The MBHp was micro-dissected and collected for RNA-seq.

(B) Hierarchical clustering of differentially expressed genes (DEGs) across groups

(C) Venn diagram showing number of DEGs comparing groups.

(D) Recovered DEGs (rDEGs) associated with reproduction and/or development processes (gene ontology/GO terms 0000003 and 0032502, respectively). "rDEGs undefined" are selected genes whose expression was not recovered when PMv and Arc were individually analyzed.

(E) rDEGs are genes with recovered expression in PMv or Arc following leptin administration.

(F) "rDEGs undefined" are selected genes whose expression was not recovered when PMv and Arc were individually analyzed.

One-way ANOVA followed by Tukey's test were used. a, b, and c: different superscripts indicate $p < 0.05$. Scale bar: 400 μm. See also Figure S1 and Table S1.

Fezf1, *Nr5a1*, *Nr4a2*, *Inhba*, *Ddc*, *Anxa1*, and *Trmt11* (Day et al., 2017; Hou et al., 2017; Topaloglu, 2017). Similarities with GWAS data on age at menarche were also noticed in pathway analyses, such as neuronal development and PI3K signaling (Day et al., 2017).

Following 2 days of leptin administration, the expression of 333 DEGs in Lep^{ob} females recovered to WT levels, which we refer to as recovered DEGs (rDEGs, Table S1). The rDEGs are genes whose expressions between Lep^{ob} and WT (±1.5fc, $q < 0.05$) were not different from those seen between WT and Lep^{ob} + leptin. Functional enrichment analysis using VLAD showed that the rDEGs were primarily annotated to developmental process, anatomical structure development/morphogenesis, cell differentiation/development/proliferation, reproductive process, ion transport and vascular development (e.g., *Shh*, *Wnt7a*, *Serpine1*, *C2*, *Vwf*, *Igfbp2*, *Eln* and, *Cpa4*). The rDEGs were mainly observed in the extracellular compartment, membrane-bounded vesicle, and plasma membrane (e.g., *Adamts4*, *Col1a2*, *Col5a3*, *Ptk2b*, *Ramp3*, *Shisa8*, and *Omd*) and were associated with ion, receptor and DNA binding, and transmembrane

transporter activity (MF). Using KEGG analysis, we found that the rDEGs were annotated to extracellular matrix-receptor interaction, protein digestion and absorption, GnRH, and estrogen signaling (Figures S1F and S1G and Table S1). About 35% of the rDEGs were associated with reproduction and/or development process (Figure 1D). Because the Lep^{ob} + leptin mice showed puberty onset right before euthanasia, we predict a subset of the rDEGs are downstream targets of leptin's facilitatory action in pubertal development and obesity-induced early puberty.

To validate our findings, the choice of cutoff values for differences, and to define whether rDEGs were part of the PMv or Arc transcriptome, we performed qPCR in micro punches of PMv and Arc from mice subjected to the same experimental design (i.e., WT, Lep^{ob}, Lep^{ob} + leptin). We selected a group of genes that were associated with reproductive and developmental processes, showed full recovery after leptin treatment, have not been previously described, and did not show high differences in fragments per kilobase of exon model per million reads mapped (FPKM) or fold changes (Figure 1D). Most of the selected genes showed recovered expression (rDEGs) in the PMv (e.g., *Shh*, *Wnt7a*, *Gipr*, *Ccl17*, *Shox2*, *Zglp1*, and *Pla2g3*) and a few in the Arc (e.g., *Rbp4* and *Zbtb16*; Figure 1E). Several rDEGs were expressed in both nuclei (e.g., *Lhx9*, *Cd46*, *Nanos2*, *Pdim3*, and *Nr4a2*). In those cases, potentially due to regulation in opposite directions, we were unable to detect differences when PMv and Arc were individually analyzed by qPCR (Figure 1F).

PMv and Arc LepRb Cell-Specific Transcriptional Changes Induced by Short-Term Leptin Treatment

LepRb neurons comprise only a subset of all cells in both PMv and Arc (Campbell et al., 2017; Cravo et al., 2013; Lam et al., 2017; Leshan et al., 2009). Thus, changes of gene expression in cells other than LepRb neurons may have masked changes in key transcripts directly associated with leptin action. To determine transcriptional changes in neurons directly targeted by leptin, we harvested RNA from LepRb cells by TRAP (Heiman et al., 2014) and performed RNA-seq (TRAP-seq). The $LepRb^{eGFP-L10a}$ mice, which express a chimeric L10a ribosomal subunit fused to enhanced green fluorescent protein (eGFP-L10a), allow for eGFP immunoprecipitation of ribosomes with associated mRNAs specifically from LepRb neurons (Allison et al., 2015, 2018). This strategy enables the identification of actively transcribed mRNAs derived from PMv or Arc LepRb neurons in response to leptin administration. Lep^{ob}_$LepRb^{eGFP-L10a}$ mice were treated with vehicle (saline) or leptin as described previously, with the exception that tissue was collected by micro punches and LepRb cell-specific RNA was isolated by TRAP (Figure 2A). WT_$LepRb^{eGFP-L10a}$ diestrous females treated with saline were used as control. Much the same as before, four injections of leptin (2 days) to Lep^{ob} females decreased body weight and induced puberty onset (vaginal opening). One hour after the last leptin or saline injection, PMv and Arc micro punches were collected from 12 mice per group. Six PMv micro punches (bilateral) and three Arc micro punches (midline) from three mice were pooled together comprising one biological replicate for a total of four biological replicates/group (Figure 2A). Taqman qPCR was used to assess *Lepr* mRNA enrichment in LepRb-enhanced versus LepRb-depleted RNAs before RNA-seq as an initial quality control. Enrichment of *Lepr* in TRAP mRNA from LepRb-enhanced samples was detected (Figure 2B; fold enrichment = 6.66 ± 0.33 for PMv and 4.56 ± 0.15 for Arc), similar to previous report using hypothalamic blocks (Allison et al., 2015). Hierarchical clustering analysis showed a clear segregation between actively translated genes in the PMv and Arc LepRb neurons (Figure 2C), revealing a functional dissociation between PMv and Arc, as previously suggested (Donato et al., 2011; Egan et al., 2017).

As an additional control, enrichment analysis was performed comparing data from a published database using TRAP-seq and the same mouse line (i.e., $LepRb^{eGFP-L10a}$ Lep^{ob} versus $LepRb^{eGFP-L10a}$ WT) (Allison et al., 2015, 2018). LepRb-enriched genes (beads FPKM/supernatant FPKM >1.5 = 1.5fc) were compiled and matched with the present data. The actively transcribed genes in LepRb neurons between experimental groups and both hypothalamic nuclei (PMv and Arc) were obtained using the same criteria as before ($\pm$1.5fc, $q < 0.05$).

In PMv LepRb neurons, 154 differentially expressed genes (TRAP_DEGs) were identified comparing Lep^{ob} and WT females (Figure 2D), of which 37 (24%) were upregulated and 117 (76%) were downregulated in Lep^{ob} mice (Figure S2A and Table S2). Enrichment analysis narrowed those numbers down to 84 LepRb-enriched DEGs, 10 upregulated (12%) and 74 downregulated (88%) in Lep^{ob} mice (Figure 2E). The upregulated TRAP_DEGs in the PMv of Lep^{ob} mice were mainly associated with cell development and adhesion

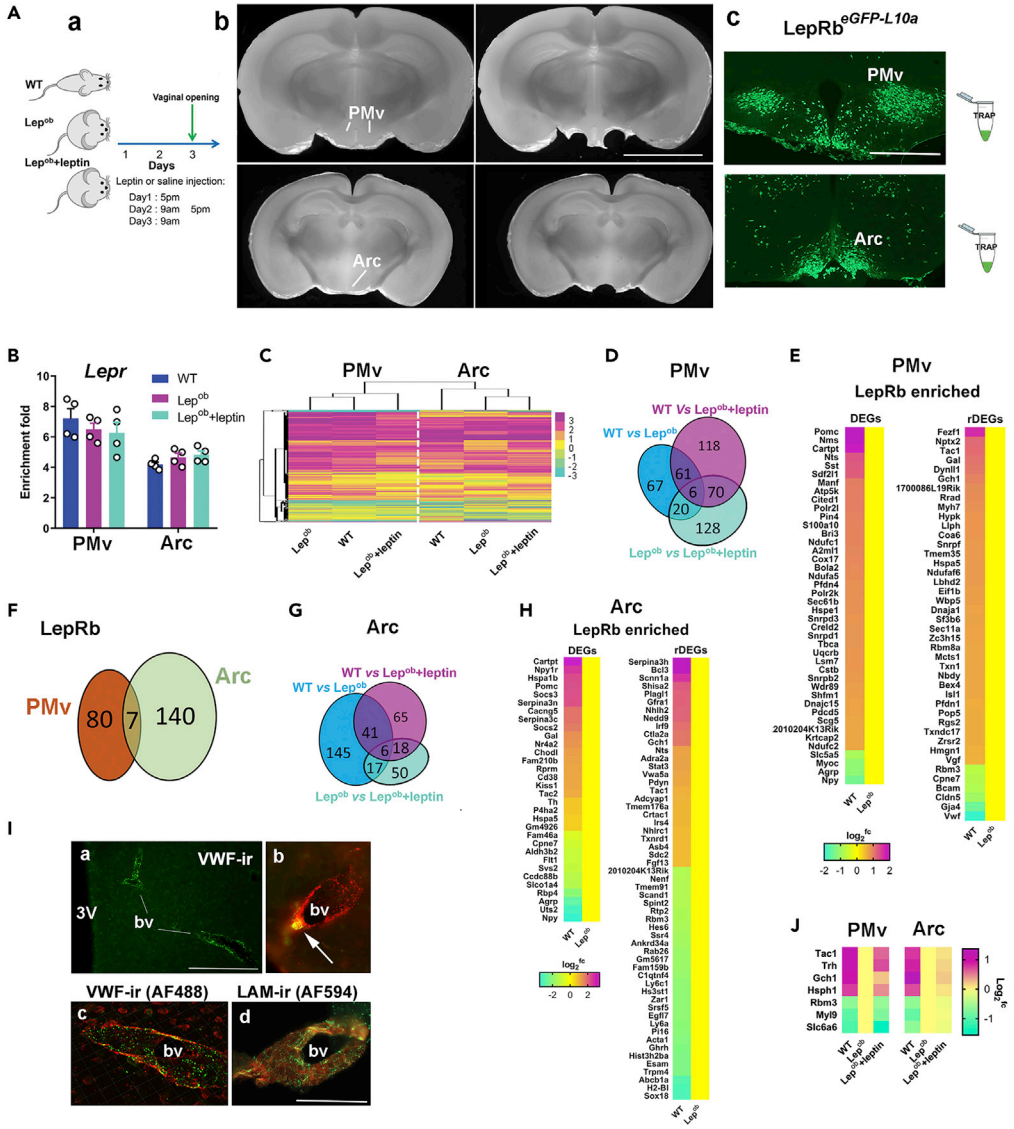

Figure 2. PMv and Arc LepRb Cell-Specific Transcriptional Changes Induced by Short-Term Leptin Treatment

(A) LepRb eGFP-L10a mice were divided into three groups: diestrous females treated with i.p. saline (WT) and Lep^{ob} females treated with i.p. saline (Lep^{ob}) or i.p. leptin (Lep^{ob} + leptin). Mice were euthanized 1 h after the last saline or leptin injections. PMv (left and right sides) and Arc (median line) were collected by micro punches (1.25 mm diameter) of individual mouse brains and LepRb_TRAP genes were subjected to RNA-seq. GFP fluorescence (green) shows the dense distribution of LepRb neurons in the PMv and Arc.

(B) Enrichment fold of *Lepr* in individual samples was used as control.

(C) Heatmap showing DEGs across treatment groups.

(D, F, and G) Venn diagrams showing number of DEGs comparing treatment groups in LepRb PMv (D) and Arc (G) neurons, and the number of recovered DEGs (rDEGs) in both nuclei (F).

(E and H) Enriched rDEGs in PMv (E) and Arc (H).

(I) Single (a and b) and dual (c and d) label immunofluorescence showing VWF immunoreactivity in endothelia of blood vessels (bv) in the brain parenchyma (a–c) and in the base of the brain (d). Blood vessels were labeled with anti-laminin in red, and VWF-ir was labeled in green (in a, c, and d). In b, GFP autofluorescence was visualized in green and VWF-ir in red. Arrow indicates a LepRb eGFP-L10a cell (GFP autofluorescence).

(J) rDEGs in both nuclei.

Scale bars: 400 μm in (A); 200 μm in (Ia), and 50 μm in (Ib, Ic, and Id). See Figures S2–S4 and Tables S2 and S3.

(e.g., *Gja4*, *Bcam*, *Cldn5*), intracellular signal transduction, and tissue remodeling. The downregulated TRAP_DEGs were clustered into cell communication, protein folding and assembly, hormone secretion, neuropeptide signaling (e.g., *Tac1*, *Nms*, *Npvf*, *Scg5*, *Nts*), mRNA processing, and oxidative phosphorylation (e.g., *Ndufaf2*, *Ndufaf6*, *Ndufc1*, *Uqcrb*) (Table S2). TRAP_DEGs were commonly observed in the extracellular space, neuron projection, and somatodendritic compartment, and were associated with receptor and protein binding and hormone activity (e.g., *Cryab*, *Fbxo2*, *Flna*, *Nptx2*, *Nts*, *Rbm3*, *Rgs11*, *Snca*, *Tac1*, *Txn1*, *Vgf*). KEGG pathways analysis showed that upregulated DEGs were selectively annotated into focal adhesion (e.g., *Vwf*, *Cav2*, *Flna*, *Myl9*), whereas downregulated DEGs were predominantly annotated into spliceosome, oxidative phosphorylation, protein processing in the endoplasmic reticulum (ER) (e.g., *Pfdn1*, *Hspe1*, *Pfdn4*, *Chordc1*, *Hspa5*), and protein export (Table S2). Several of the PMv DEGs have been described in GWAS and transcriptome studies associated with reproductive control, e.g., *Tac1*, *Pin4*, *Tbca*, and *Fezf1* (Day et al., 2017; Hou et al., 2017; Maguire et al., 2017; Simavli et al., 2015).

Following leptin administration, the expression patterns of 87 DEGs (56.5% of total 154) and 42 LepRb-enriched DEGs (50% of 84) in the PMv of Lep^{ob} females were similar to that seen in WT mice (TRAP_rDEGs, Figures 2E, 2F, and S2B). They were assembled into regulation of cell communication and development, nervous system development, neurogenesis, response to hormone, morphogenesis, protein folding, cytoskeleton organization, and secretion (Table S2). They were annotated into extracellular region, neuron projection, somatodendritic compartment, membrane-bounded and extracellular vesicles (CC), receptor and protein binding, hormone activity, and unfolded protein binding (MF). KEGG pathway analysis highlighted protein processing in the ER (Figures S2C and S2E; Table S2). As observed in previous experiments, only part of the DEGs in Lep^{ob} mice was recovered to WT levels (rDEGs). Because puberty onset was observed in leptin-treated Lep^{ob} mice, we predict that the rDEGs are those preferentially associated with leptin action in pubertal maturation and obesity-induced advance in puberty.

In Arc LepRb neurons, 209 TRAP_DEGs were identified between Lep^{ob} and WT mice (Figures 2G); 38.8% were greater in Lep^{ob} and 61.2% were greater in WT females (or downregulated in Lep^{ob}; Figure S3A; Table S3). LepRb enrichment analysis showed that 87 DEGs were enriched in Arc_LepRb neurons (Figure 2H). The downregulated TRAP_DEGs in Lep^{ob} were predominantly annotated into signal transduction, hormone and neuropeptide signaling (e.g., *Cartpt*, *Pomc*, *Gal*, *Kiss1*, *Tac2*, *Npvf*, *Pdyn*, *Adcyap1*, *Gfra1*), developmental process, neurogenesis, anatomical structure morphogenesis, protein kinase activity, and blood circulation. They were mostly assembled into extracellular region, neuron projections, somatodendritic compartment, and signaling receptor. The upregulated TRAP_DEGs were mainly categorized into morphogenesis, vasculogenesis (e.g., *Apold1*, *Gja4*, *Flna*, *Vwf*) and cell motility (e.g., *Acta1*, *Flt1*, *Egfl7*, *Trpm4*) (Table S3), cytoskeleton, and extracellular space, and were associated with protein heterodimerization and peptidase inhibitor activity. KEGG pathways analysis assembled the upregulated TRAP_DEGs into protein processing in ER adipokine, MAPK, and prolactin signaling, whereas the downregulated TRAP_DEGs were mainly annotated to leukocyte trans-endothelial migration (Table S3).

In the Arc, the expression of 147 DEGs (70% of 209) and 55 LepRb-enriched DEGs (63% of 87) in Lep^{ob} females reached the WT levels after leptin treatment (rDEGs; Figures 2F and S3B). The TRAP_rDEGs were mainly annotated into regulation of cell communication, carbohydrate derivative metabolism, hormone transport and secretion, and blood circulation (e.g., *Sox18*, *Egfl7*, *Thy1*, and *Vwf*). The *Vwf* gene is part of endothelial cells transcriptome (Yamamoto et al., 1998) and has been consistently found in LepRb cell-specific TRAP-seq (Figure 2I) (Allison et al., 2018). Sporadic LepRb GFP-labeled cells were observed in the adjacencies of blood vessels (Figure 2I), but single-cell RNA-seq has indicated that *Vwf* is also expressed by neurons (Zeisel et al., 2018). Further studies will be necessary to assess if *Vwf* is expressed in LepRb neurons or whether the data result from endothelial cell contamination of the TRAP procedure. Either way, *Vwf* is regulated by acute leptin actions and may be associated with vasculogenesis during pubertal maturation.

Arc TRAP_rDEGs were enriched in the soma, axon, cell junction, and somatodendritic compartment, and in hormone activity and kinase and receptor binding (Figures S3C–S3E). KEGG pathway analysis shows that these acute TRAP_rDEGs were notably enriched in protein processing in ER(Figures S3C–S3E; Table S3). Several of the Arc rDEGs have been described in GWAS and transcriptome studies associated with reproductive control, e.g., *Tac1 and Tac2*, *Kiss1*, *Nr4a2*, *Pin4*, *Fndc3b*, *Gpr83,* and *Nedd1* (Day et al., 2017; Hou et al., 2017; Maguire et al., 2017; Simavli et al., 2015).

We found seven leptin-responsive TRAP_rDEGs expressed in both PMv and Arc (Figures 2F and 2J), of which four were higher following leptin treatment (WT; *Tac1*, *Trh*, *Hsph1*, and *Gch1*) and three were higher in the absence of leptin (Lep^{ob}; *Rbm3*, *Myl9*, and *Slc6a6*). Of those, *Tac1*, *Gch1*, and *Rbm3* were previously described to be enriched in hypothalamic LepRb neurons (Allison et al., 2015, 2018). A number of described genes highly expressed and regulated by leptin in LepRb neurons were also identified as TRAP_DEGs or TRAP_rDEGs, e.g., *Pomc*, *Agrp*, *Npy*, *Cartpt*, *Socs3*, *Nts*, and *Ghrh* (Ahima et al., 1999; Allison et al., 2015, 2018; Mizuno and Mobbs, 1999), indicating the efficiency of TRAP-seq to detect LepRb-specific transcripts.

The LepRb triggers cellular responses through several molecular pathways (Bates et al., 2003; Elias and Purohit, 2013; Morris and Rui, 2009; Myers et al., 2008; Singireddy et al., 2013). The JAK-STAT signaling via phosphorylation of signal transducer and activator of transcription 3 and 5 (pSTAT3 or pSTAT5) is well described. Using CiiiDER software (Gearing et al., 2019) we searched for DEGs in LepRb neurons with potential binding sites for pSTAT3 and pSTAT5. Promoter regions spanning 1,500 bp upstream and 500 bp downstream of the transcription start site were identified. Both PMv and Arc showed a series of DEGs with putative pSTAT3 and pSTAT5 binding sequences. Enrichment analysis using 1,000 genes with no expression changes (fold change = 0) as background identified several statistically enriched genes only for pSTAT5 binding in the PMv LepRb neurons, e.g., *Ctss*, *Gpr88*, *Hhatl*, *Hsph1*, *Phyhd1*, *Rbm3*, *Tgm2*, *Trh*, and *Nptx2*. Due to the small number of genes with STAT3- or STAT5-binding sites, we predict that most of leptin's effect in the reproductive axis is attained by alternative signaling pathways, such as PI3K (Day et al., 2017; Garcia-Galiano et al., 2017). This is in agreement with previous studies suggesting that JAK-STAT signaling has only minor effects in mediating leptin's action in reproductive physiology (Bates et al., 2003; Bjornholm et al., 2007; Singireddy et al., 2013).

To further validate and assess the specificity of both RNA-seq data, rDEGs in MBHp and leptin-induced TRAP_DEGs in PMv and Arc LepRb neurons, we performed overlapping analysis with previously identified genes (2,736) enriched in LepRb-expressing cells (Allison et al., 2015, 2018). We found that 133 of 562 DEGs in the MBHp transcriptome were LepRb-enriched genes. Of them, 68 were rDEGs (Figure S4A).

Comparing previously identified hypothalamic transcripts that are both LepRb neuron enriched and leptin regulated (364) in MBHp, we found that 17 (e.g., *Rbm3*, *Vwf*, *Ccl17*, *Rbp4*, *Bst1*, *Lamc2*, *Cpa4*, *Ghsr*, *Fgl2*, *Fosl2*, *Atf3*, and *Prokr2*) were acutely regulated by leptin (Figure S4B). In PMv LepRb neurons 13 (e.g., *Rbm3*, *Vwf*, *Gch1*, *Tac1*, *Cldn5*, *Rgs2*, *Llph*, and *Dnaja1*) were both LepRb cell enriched and acutely regulated by leptin. In Arc LepRb neurons 19 (e.g., *Rbm3*, *Gch1*, *Tac1*, *Ghrh*, *Irs4*, *Stat3*, *Irf9*, *Bcl3*, *Ly6a*, *Nts*, and *Serpina3h*) were both LepRb-neuron-enriched and leptin-regulated genes (Allison et al., 2018). This comparative analysis, although informative, should be interpreted with caution as methodological differences are apparent. For instance, previous studies have used one leptin injection and transcript enrichment comparing RNA levels in immunoprecipitated versus supernatant, whereas we have used four leptin injections comparing immunoprecipitated across treatment groups. Thus, it is possible that four leptin injections may have induced the expression of genes undetected in previous studies. Because we have not performed a direct enrichment analysis, we used only genes described in a published database known to be enriched in LepRb neurons. Further studies will be necessary to validate the enrichment of genes in LepRb neurons not previously described.

We also identified 13 TRAP_DEGs in Arc LepRb neurons reported to be expressed in AgRP neurons and to be regulated by fasting (Henry et al., 2015). Of those, *Rbm3*, *Hs3st1*, *Gch1*, *Nts*, *Irf9*, and *Plagl1* were LepRb neuron enriched and acutely regulated by leptin (Figure S4C) (Allison et al., 2015, 2018). Due to the role of AgRP neurons in the metabolic control of pubertal development (Egan et al., 2017; Padilla et al., 2017), we postulate those DEGs have key roles in obesity (leptin)-induced advance in puberty.

PMv and Arc Transcriptional Changes during Pubertal Transition in Wild-Type Female Mice

To dissociate the metabolic and reproductive effects of leptin treatment and further define if the identified DEGs in obese mice are physiologically relevant in typical pubertal development, we evaluated the transcriptomic changes in the PMv and Arc of WT mice comparing prepubertal (PP) at postnatal day 18 (P18) and diestrous females (Di) at P60–70. P18 was defined based on previous publications showing that developmental changes in the hypothalamic transcriptome are abundant between P12 and P22 (Hou et al., 2017).

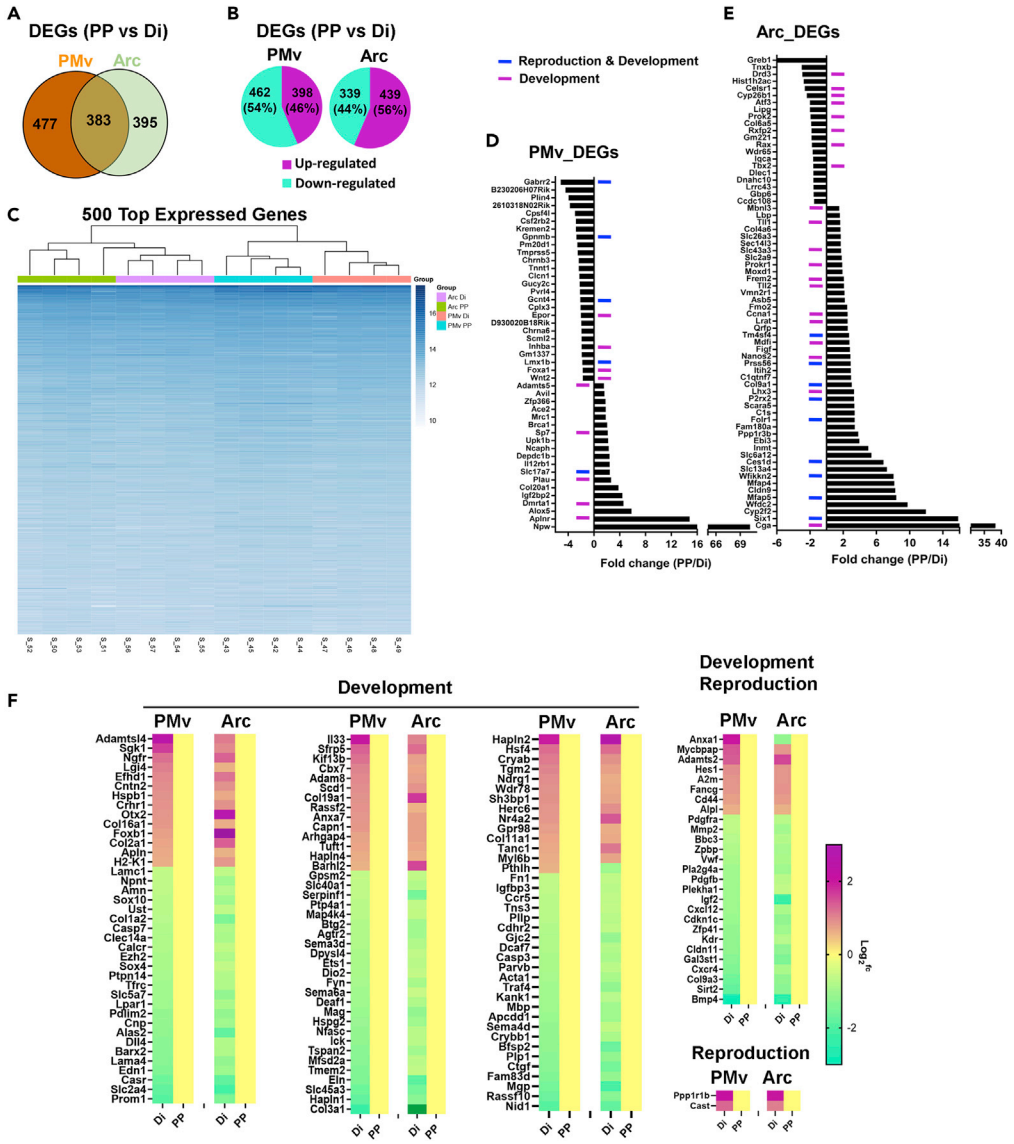

Figure 3. PMv and Arc Transcriptional Changes during Pubertal Transition in Wild-Type Female Mice

(A) Venn diagram of differentially expressed genes (DEGs) in PMv and Arc between prepubertal (PP) and diestrous (Di) females.

(B) Amount and percentage of up- and downregulated DEGs.

(C) Hierarchical clustering of the top 500 expressed genes.

(D and E) DEGs between PP and Di mice expressed (D) only in the PMv or (E) only in the Arc. Blue lines: genes associated with both reproduction and development. Purple lines: genes associated with development.

(F) Heatmap showing relative gene expression of common DEGs in the PMv and Arc enriched in development and reproduction (GO 0032502 and 0000003, respectively).

See Figure S5 and Table S4.

PMv and Arc micro punches were collected as previously described (n = 4 biological replicates/group), and total transcripts were submitted to RNA-seq analysis.

Using the same criteria to determine differences described in previous sections (±1.5fc, $q < 0.05$), we found 860 DEGs in PMv samples between PP and Di females (Figure 3A). Of those, 398 (46%) were upregulated and 462 (54%) were downregulated in PP (Figure 3B; Table S3). In Arc samples, 778 DEGs were identified (Figure 3A), of which 439 (56%) were upregulated and 339 (44%) were downregulated in PP (Figure 3B; Table S3). There were 383 DEGs common to both PMv and Arc, 477 were represented in PMv samples only and

395 in Arc samples only (Figure 3A). Hierarchical clustering of the top 500 genes showed a clear segregation of transcript profile between PMv and Arc, and between PP and Di within PMv and Arc (Figure 3C), suggesting a functional dissociation between both nuclei during pubertal transition in wild type females.

Functional enrichment analysis showed that the upregulated DEGs in PMv of PP females were predominantly enriched in development, cell adhesion and migration, cell communication and signaling, reproductive process, and angiogenesis (Figure S5A; Table S4). They were highly represented in plasma membrane, extracellular space, cell junction, neuron projection, and somatodendritic compartment, and enriched in transporter activity, protein complex, and carbohydrate binding. In contrast, the downregulated DEGs in PMv were predominantly enriched in development, morphogenesis, transport and neurogenesis, in cytoskeleton, ion binding, protein dimerization activity, and transcription factor activity (Figures S5B and S5C; Table S4). KEGG analysis of upregulated DEGs included pathways in cancer, PI3K-Akt signaling, focal adhesion, extracellular matrix-receptor interaction, chemokine signaling, and protein processing (Table S4). Of the total PMv DEGs (860), only about 2.5% (22 genes) were previously associated with disorders of pubertal development or IHH, including *Mkrn3*, *Sox10*, *Irx3*, *Igf2bp2*, *Otx2*, *Calcr*, *Inhba*, *Fezf1*, *Cbx4*, *Cbx7*, and *Nr4a2* (Abreu et al., 2013; Day et al., 2017; Hou et al., 2017; Topaloglu, 2017).

In the Arc of PP female mice, the upregulated DEGs were predominantly associated with development, morphogenesis, transport, neurogenesis, reproductive process, cell proliferation, cell adhesion, growth factor, vasculogenesis, and axon ensheathment. They were mainly observed in cell periphery, plasma membrane, extracellular region, and cytoskeleton and were associated with enzyme regulator activity, ion transmembrane transporter activity, cell adhesion, and receptor and growth factor binding. Downregulated DEGs were predominantly associated with development, cell differentiation and communication, morphogenesis and neurogenesis, and in MF associated with ion, lipid, and cofactor binding and transcription factor activity (Figures S5D–S5F; Table S4). KEGG pathways analysis highlighted gene enrichment in PI3K signaling, focal adhesion, Ras signaling, protein processing and TGFβ signaling, and de-enrichment in metabolic pathways and arginine biosynthesis. Of the total Arc_DEGs (778), about 4% (29 genes) were previously associated with disorders of pubertal development or IHH, including *Mkrn3*, *Tac2*, *Tacr3*, *Prok2*, *Prokr2*, *Sim1*, *Otx2*, *Lhx3*, *Nr4a2*, *Anxa1*, *Cbx4*, and *Cbx7* (Abreu et al., 2013; Day et al., 2017; Hou et al., 2017; Topaloglu, 2017).

The PMv samples were slightly contaminated with cells of the Arc, as evidenced by *Agrp* and *Pomc* expression. Thus, to gain insights into the functional dissociation between PMv and Arc, we performed overlapping analysis of the expression of genes among individual samples of both nuclei. Only DEGs whose expression was detected in all individual samples of either PMv or Arc were assembled as PMv_DEGs or Arc_DEGs. The expression of 244 genes was only detected in the PMv, of which 197 were protein-coding genes based on UniProt database (Table S4). Of the 197 protein-coding genes, 45 were PMv_DEGs (Figure 3D). The expression of 531 genes was only detected in the Arc, of which 444 were protein-coding genes (Table S4) and 67 of the 444 protein-coding genes were Arc_DEGs (Figure 3E). Functional enrichment analysis showed that most of these selectively and differentially expressed genes in the PMv or in the Arc were associated with development and/or reproduction. Five PMv_DEGs (*Gabrr2*, *Gpnmb*, *Gcnt4*, *Lmx1b*, and *Slc17a1*) and 9 Arc_DEGs (*Six1*, *Mfap5*, *Wfikkn2*, *Ces1d*, *Folr1*, *P2rx2*, *Col9a1*, *Prss56*, and *Tm4sf4*) were associated with both development and reproduction (Figures 3E and 3F). Except for *Slc17a7* in the PMv, DEGs associated with development and reproduction were upregulated in the Arc and downregulated in the PMv of PP mice. This is particularly interesting as LepRb neurons in the PMv and Arc associated with pubertal development are differentially regulated by leptin (Donato et al., 2011; Egan et al., 2017; Padilla et al., 2017; Ross et al., 2018; Williams et al., 2011).

A significant number of DEGs (383) were expressed in both PMv and Arc. Of those, about 40% were associated with reproduction and/or developmental process and, except for *Anxa1* and *Pthlh*, showed same direction of changes (up- or downregulation) comparing PP and Di (Figure 3F). Of note, around 20% of the DEGs were associated with the extracellular region (e.g., *Lamc1*, *Lama4*, *Col9a3*, *Serpinf1*, *Hapln2*, *Admtsl4*).

Overlapping Analysis of all RNA-Seq Data Focused on the PMv

We next performed overlapping analyses of the DEGs between Lep^{ob} and WT mice obtained in the MBHp RNA-seq, in the LepRb TRAP-seq (PMv DEGs and Arc DEGs), and in the PP versus Di RNA-seq. Only DEGs

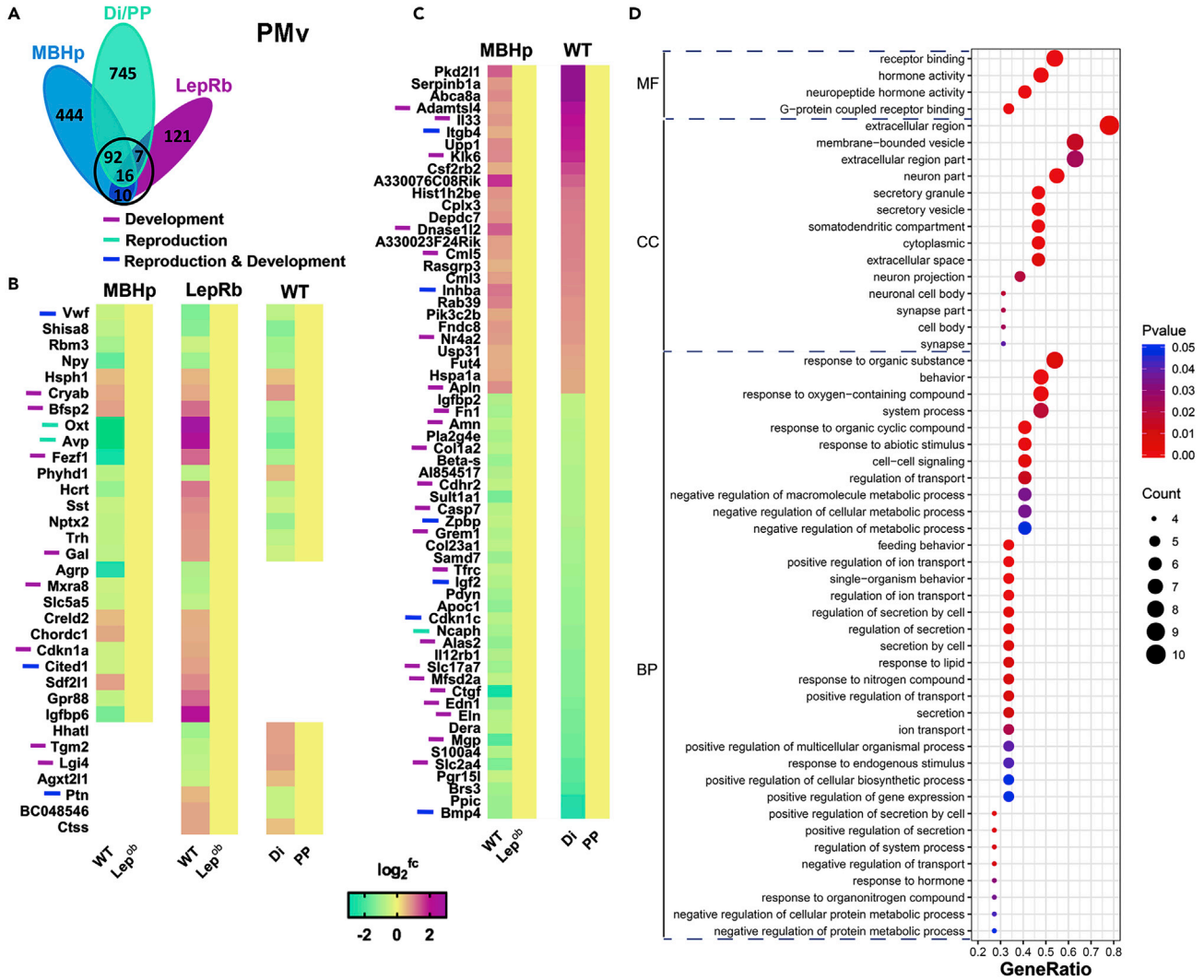

Figure 4. Overlapping Analysis of all RNA-Seq Data Focused on PMv

(A) Venn diagram showing independent and overlapping DEGs between Lep^{ob} and WT mice obtained in the MBHp RNA-seq, in the LepRb TRAP-seq (PMv_DEGs), and DEGs between PP and Di RNA-seq.

(B) Heatmap showing relative gene expression comparing MBHp RNAseq, LepRb TRAP-seq (PMv_DEGs) and PP vs. Di RNAseq (PMv_DEGs).

(C) Heatmap showing relative gene expression comparing MBHp RNAseq and PP vs. Di RNAseq (PMv_DEGs).

(D) Molecular function (MF), cellular component (CC), and biological process (BP) of shared DEGs using DAVID enrichment analysis.

were compared to gain insights into common transcriptome programs between prepubertal (wild-type and Lep^{ob} with no leptin treatment) and adult female mice. Genes expressed in at least two datasets showing expression in the same direction relative to PP versus Di were named "core" DEGs and were used for GO enrichment analysis. With this strategy, we were able to identify genes directly or indirectly associated with leptin action and those associated with pubertal development, including potential leptin downstream targets.

In the PMv, a core of 125 DEGs was assembled (Figure 4A). Of those, 16 DEGs were common in all three RNA-seq data and 6 were modulated in the same direction (*e.g.*, *Vwf*, *Shisa8*, *Rbm3*, *Npy*, *Hsph1*, *Cryab*) (Figure 4B). Contamination by the Arc is evident as *Npy* was detected in all three experiments. Ten genes were common DEGs in MBHp RNA-seq and TRAP-seq (*Mxra8*, *Slc5a5*, *Creld2*, *Chordc1*, *Cdkn1a*, *Cited1*, *Sdf2l1*, *Gpr88*, *Igfbp6*) but not in the pubertal transition, suggesting they are associated with leptin physiology but may have low relevance for typical pubertal development in wild-type mice. Seven DEGs were only detected in PMv TRAP-seq neurons and PP versus Di RNA-seq. Except for *Ctss*, all of them were

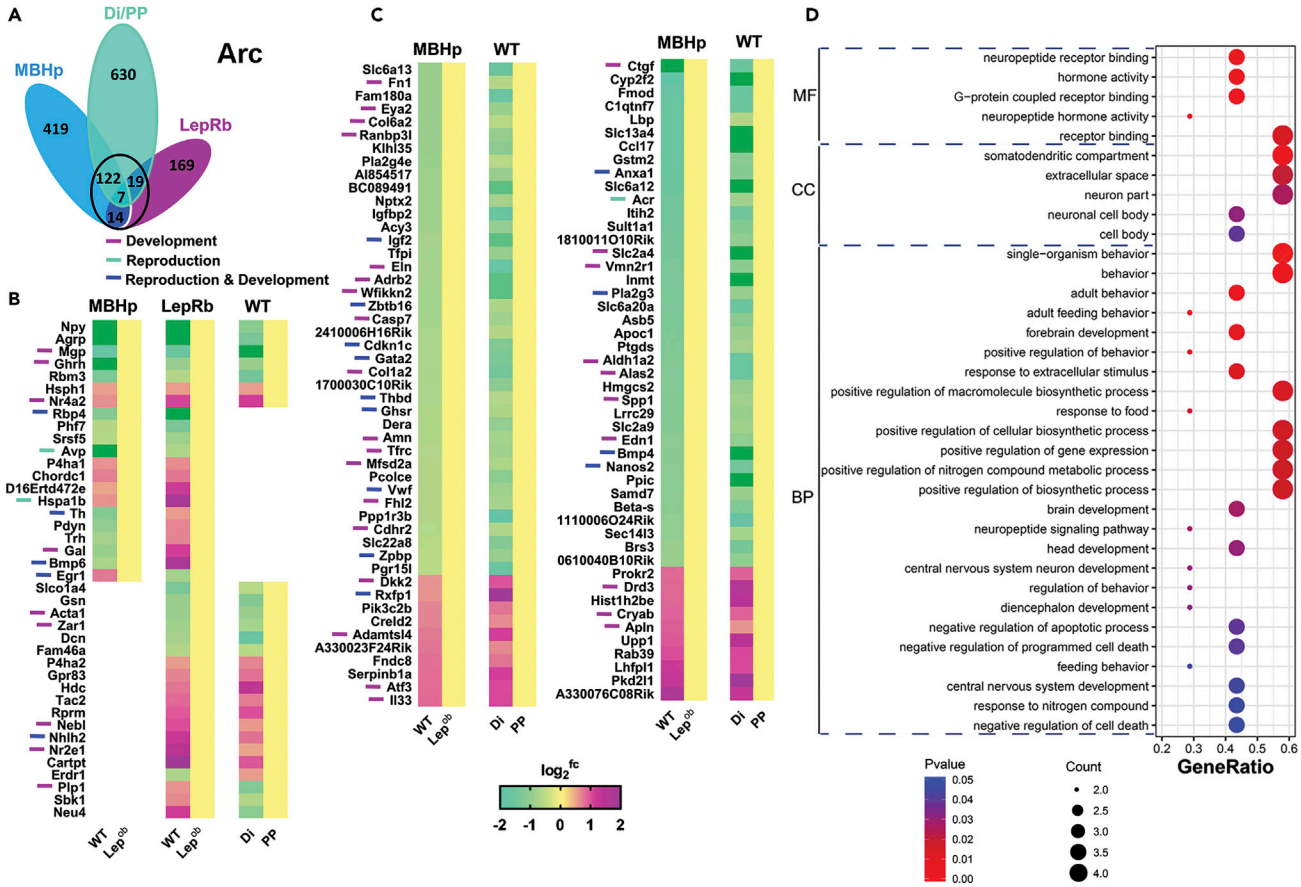

Figure 5. Overlapping Analysis of all RNA-Seq Data Focused on Arc

(A) Venn diagram showing independent and overlapping DEGs between Lep^{ob} and WT mice obtained in the MBHp-RNA-seq, in the LepRb TRAP-seq (Arc_DEGs), and between PP and Di RNA-seq.

(B) Heatmap showing relative gene expression comparing MBHp RNAseq, LepRb TRAP-seq (Arc_DEGs) and PP vs. Di RNAseq (Arc_DEGs).

(C) Heatmap showing relative gene expression comparing MBHp RNAseq and PP vs. Di RNAseq (Arc_DEGs).

(D) Molecular function (MF), cellular component (CC), and biological process (BP) of shared DEGs using DAVID enrichment analysis.

regulated in opposite directions. The significance of this finding is not evident but may suggest a distinct response to different levels of leptin. The other 92 genes were DEGs in MBHp and in PP versus Di RNA-seq, of which 70% were regulated in the same direction (Figure 4C) and may comprise downstream targets associated with leptin action in pubertal development. Functional enrichment analysis highlighted high association with extracellular space, membrane-bounded vesicle, receptor binding, and behavior among others (Figure 4D).

Overlapping Analysis of all RNA-Seq Data Focused on the Arc

In the Arc, a core of 162 DEGs was identified (Figure 5A), of which 7 (*Npy*, *Agrp*, *Mgp*, *Ghrh*, *Rbm3*, *Hsph1* and *Nr4a2*) were common in all three RNA-seq data. Fourteen DEGs were common in MBHp RNA-seq and TRAP-seq (Figure 5B). Of those, 8 showed expression changes in the same direction (i.e., *Rbp4*, *Phf7*, *Srsf5*, *Avp*, *P4ha1*, *Chordc1*, *D16Ertd472e*, and *Hspa1b*). The other 122 genes were DEGs in MBHp and PP versus Di RNA-seq, of which 78% were coordinately regulated (e.g., *Igf2*, *Cdkn1c*, *Gata2*, *Anxa1*, *Pla2g3*; Figure 5C). We predict that those DEGs are downstream targets of leptin. Functional enrichment analysis revealed enrichment in receptor binding and somatodendritic and extracellular spaces and positive regulation of biosynthetic processes among others (Figure 5D).

Common GO subcategories are apparent comparing both hypothalamic nuclei. Of note, DEGs associated with receptor binding and hormone activity, extracellular space, and somatodendritic compartment are highly represented. The former subcategories are predictable, whereas only a few studies have

investigated the role of glial components and somatodendritic remodeling in pubertal development (Clasadonte and Prevot, 2018; Cottrell et al., 2006; Prevot et al., 2003). Our findings highlight the relevance of neuropil organization, vasculogenesis, and extracellular matrix composition in leptin-induced and typical pubertal maturation.

Protein-Protein Interaction (PPI) and a Network Model for Leptin Action in Puberty Onset via the PMv

The PPI network using only the central core genes (125 in the PMv and 162 in the Arc, Figures 4 and 5) regulated in the same direction in all three RNA-seq assays was built using STRING v.11 (Search Tool for the Retrieval of Interacting Genes/Proteins) and visualized using Cytoscape software v.3.7.2 (Figures 6 and 7). Nodes in the first connection with *Lepr* (e.g., *Vwf*, *Cryab*, *Rbm3*, *Hsph1*, and *Shisa8* in the PMv, and *Agrp*, *Npy*, *Cart*, *Ghrh*, *Rbm3*, *Hsph1*, *Nr4a2*, and *Mgp* in the Arc) represent genes predicted to be direct targets of leptin with a role in pubertal development. Nodes in the second connection with *Lepr* are common DEGs in MBHp RNA-seq and PP versus Di RNA-seq, but not TRAP-seq. These are genes experimentally predicted by STRING software to be downstream targets of leptin in pubertal development in undefined cells. Nodes in the third connection represent DEGs between PP and Di experimentally determined by STRING to interact with targets of leptin in pubertal development (Figures 6 and 7). Among them, *Bcl11*, *Ctsk*, *Sox10*, *Mkrn3*, *Kctd13*, and *Prokr2* are genes previously described to have a role in pubertal development and/or fertility (Day et al., 2017; Hou et al., 2017; Topaloglu, 2017). We predict that DEGs in the first node are directly regulated by changing levels of leptin and could potentially mediate part of obesity-induced early puberty (Biro et al., 2006; Castellano et al., 2011; Herman-Giddens et al., 1997; Lee et al., 2010; Walvoord, 2010).

Little is known about the molecular mechanisms underlying PMv neuronal actions in pubertal development. The transcriptome analyses highlighted a wealth of genes associated with synaptic strength, extracellular remodeling, and plasticity of dendritic spines. Several genes that are regulated both by leptin (WT versus Lep^{ob}) and during pubertal transition (e.g., *Bmp4*, *Ctgf*, *Col1a2*, and *Itgb4*) have been identified in direct PPI networks with several laminin subunits. Notably, during postnatal development, hippocampal neurons synthesize and deposit laminins to stabilize synapses and shape dendritic spines (Omar et al., 2017). Using a broad-spectrum antiserum for laminin subunits, we observed a dense distribution of laminin immunoreactive (Lam-ir) cells in the PMv. Colocalization between LepRb GFP and Lam immunoreactivity was higher in Lep^{ob} and in PP (about 25%) compared with Di (12%) females (Figure 6B). Moderate to low number of Lam-ir cells were also observed in the Arc, but virtually no colocalization was detected in LepRb-GFP neurons. Our findings indicate that at least part of neuropil remodeling during pubertal maturation is attained by leptin recruitment of those pathways specifically in PMv neurons.

Protein-Protein Interaction (PPI) and a Network Model for Leptin Action in Puberty Onset via the Arc

In the Arc, *Npy* and *Agrp* are well-described primary targets of leptin in metabolic and reproductive regulation (Egan et al., 2017; Padilla et al., 2017; Wójcik-Gładysz and Polkowska, 2006), whereas the role of direct leptin actions in *Ghrh* neurons is not yet clear (Rupp et al., 2018). We did not detect changes in *Kiss1* or *Pdyn*, but *Tac2* expression was lower in PP and Lep^{ob} mice. Similarly, the difference in *Pomc* was undetectable, whereas *Cartpt*, coexpressed with *Pomc* in Arc neurons, was highly regulated. In agreement with previous studies, *Cartpt* was low in PP and Lep^{ob} mice (Kristensen et al., 1998; Rodrigues et al., 2011). Arc *Cartpt* is also decreased in conditions of calorie restriction when leptin levels are low (Ahima et al., 1999; True et al., 2013). In addition to transcript levels, we found low density of CART-ir fibers in the Arc of Lep^{ob} and PP mice. Whether Arc *Cartpt* has a role in pubertal development needs further investigation.

Common Transcripts

Several transcripts were observed in PPI and network modeling of both PMv and Arc. The *Nr4a2* encodes a nuclear receptor that acts as a transcription activator or transrepressor by stabilizing histone-DNA binding (Safe et al., 2016). GWAS studies identified the *Nr4a2* (*Nurr1*) gene as a genetic locus associated with puberty timing (Day et al., 2017). Knockout mice for *Nr4a2* show deficient differentiation of dopaminergic neurons in the ventral tegmental area (Saucedo-Cardenas et al., 1998; Zetterström et al., 1997), but whether this is also associated with the development of hypothalamic dopaminergic neurons and pubertal maturation is not known. Of note, components of the dopaminergic system, including *Cdkn1c*, *Ddc*, *Slc6a3*, *Th*, *Gpr88*, and *Drd3* are highly represented in our database. In addition, regulation of *Shisa8*, a member of cysteine knot AMPA receptor-modulating proteins associated with modulation of glutamatergic

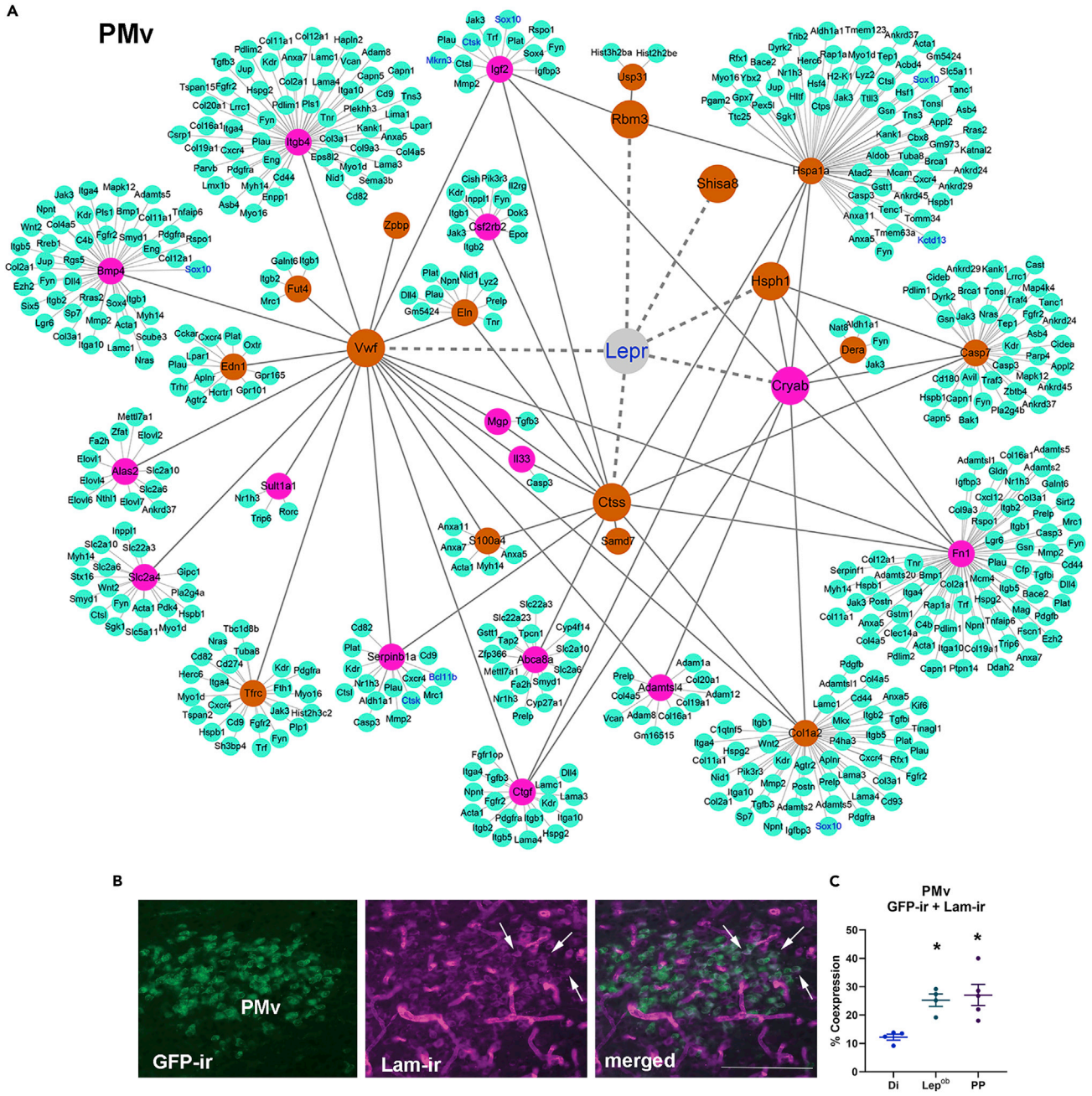

Figure 6. Protein-Protein Interaction (PPI) and a Network Model for Leptin Action in Puberty Onset via the PMv

(A) Nodes in first connection with *Lepr* are genes predicted to be direct targets of leptin. Nodes in second connection are DEGs common in MBHp and PP versus Di RNA-seq, experimentally predicted to be downstream targets of leptin. Nodes in third connection (green) represent PP versus Di DEGs experimentally determined to interact with leptin targets. Purple, DEGs; orange, rDEGs; solid lines, interactions identified by STRING; dotted lines, predicted interactions.

(B) Fluorescent images showing partial colocalization of LepRb eGFP and Laminin (Lam) immunoreactivity (-ir). Arrows indicate dual-labeled neurons. Scale bar: 200 μm.

(C) Quantification of dual-labeled neurons in the PMv of WT, Lep^{ob}, and PP females. Data are represented as mean ± SEM. One-way-ANOVA and Tukey's test were used. $F(2, 10) = 7.959$, *$p < 0.01$. .

synaptic strengths (Farrow et al., 2015), specifically in the PMv is noteworthy. PMv neurons are essentially glutamatergic and studies have implicated leptin in glutamatergic synaptogenesis of hippocampal neurons (Bland et al., 2020). Previous studies have shown that leptin action in glutamatergic PMv neurons is

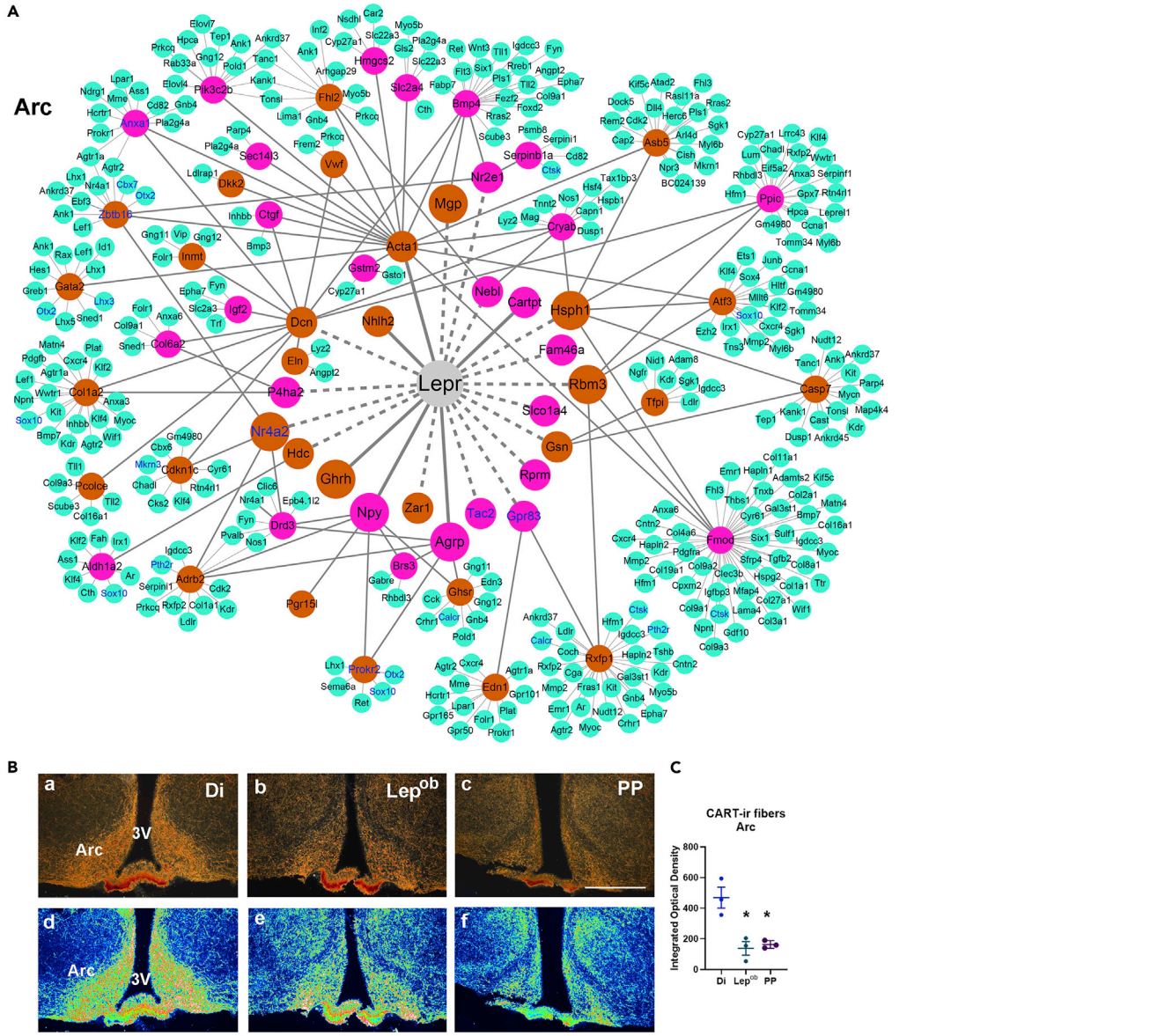

Figure 7. Protein-Protein Interaction (PPI) and a Network Model for Leptin Action in Puberty Onset via the Arc

(A) Nodes in first connection with *Lepr* are genes predicted to be direct targets of leptin. Nodes in second connection are DEGs common in MBHp and PP versus Di RNA-seq, experimentally predicted to be downstream targets of leptin. Nodes in third connection (green) represent PP versus Di DEGs experimentally determined to interact with leptin targets. Purple, DEGs; orange, rDEGs; solid lines, interactions identified by STRING; dotted lines, predicted interactions.

(B) CART immunoreactivity (-ir) in PP versus Di.

(C) Quantification of CART-ir fiber density in the Arc. Note higher density of CART-ir fibers in diestrous females compared with Lep^{ob} and PP. 3V, third ventricle. Ba–Bc, immunoperoxidase and silver amplification; Bd–Bf, pseudocolor using LUC (Zeiss) and heatmap to demonstrate fiber density. Data are represented as mean ± SEM. One-way-ANOVA and Tukey's test were used. $F(2, 6) = 14.78$, *$p < 0.01$. Scale bar: 200 μm in (Ba–Bf).

sufficient but not required for pubertal development (Donato et al., 2011; Zuure et al., 2013). Whether these findings are a result of developmental adaptations commonly seen in studies using mouse genetics or rather an evidence for redundant pathways need further evaluation.

Subnetworks derived from *Hsph1* gene are predicted in both the PMv and the Arc transcriptome. The *Hsph1* (heat shock protein family H member 1) gene is annotated to protein processing in ER. *Hsph1*

and *Hspa1a* comprise crucial molecular machinery that prevents the aggregation of misfolded protein (Mattoo et al., 2013). Protein overload or misfolded may induce ER stress and neuronal death, leading to metabolic disorders and leptin resistance (Ozcan et al., 2009; Yang et al., 2010). The effects of ER stress on pubertal development are not clear, but the fine regulation of protein production for tissue growth and differentiation is critical for sexual maturation and individual health in adult ages. Likewise, the *Rbm3* (RNA-binding motif 3) and *Cryab*, also known as *Hspb5* (small heat shock protein B5) have been associated with neurogenesis and inhibition of neurodegenerative cell death (Jackson et al., 2019). Together with the recruitment of *Vwf*, *Mgp* and downstream associated transcripts they may ensure neurite growth and differentiation, vasculogenesis, and synthesis and degradation of components of the extracellular space during pubertal development (Randi et al., 2018; Yao et al., 2016; Zhu and Reiser, 2018).

In this study, we took advantage of the possibility of monitoring pubertal development in obese mice to generate a database of genes potentially associated with leptin action in pubertal development. The TRAP-seq allowed for the dissociation of direct and potential downstream targets, and hypothalamic microdissection enabled the identification of potential processes outside neuronal soma, including vasculogenesis, remodeling of somatodendritic space, axonal growth, and extracellular space composition. We further used an RNA-seq database to compare juvenile and adult wild-type mice in the attempt to dissociate leptin's effect in metabolic and sexual maturation. Genetic screening in human subjects will further inform the relevance of the identified genes for the understanding of the physiopathology of the HPG axis development, and functional studies in animal models will be necessary to assess their role in sexual maturation and the underlying mechanisms. Of note, a subset of the DEGs were identified in humans with HH, infertility, or altered pubertal timing (e.g., homologs of *Fezf1*, *Nr5a1*, *Prok2*, *Prokr2*, *Tac2*, and *Mkrn3*) indicating that the experimental design and approaches used herein are reliable and effective. The proposed models of multi-level nodes and clustering provide a framework and insights into the molecular bases of puberty onset and the mechanisms associated with the obesity-induced advance in puberty.

Limitations of the Study

The use of the Lep^{ob} mice enabled the close monitoring of puberty onset. However, the complex metabolic, endocrine, and autonomic phenotype of these mice must be taken into consideration, and data must be interpreted with caution. We focused our analysis on genes associated with development and reproductive processes and compared the database with those obtained from lean wild-type mice. With this strategy, we expect to have identified most of the genes potentially associated with leptin action in pubertal maturation and obesity-induced advance in puberty. However, mixed data cannot be completely excluded also because puberty is a complex temporal process during which distinct physiological systems develop. The main goal of the present study was to unravel genes associated with puberty onset. Additional studies will be necessary to reveal key transcriptome programs across pubertal maturation and on puberty completion. We also anticipate that the number of relevant DEGs is under-represented due to the use of TRAP for cell-specific isolation. TRAP allows for identification of genes transcribed at the time of tissue harvesting; DEGs that are not acutely induced by leptin were left out of the analysis. Moreover, due to the heterogeneous nature of LepRb neurons, single-cell RNA-seq will be necessary to identify the subpopulations of PMv and Arc neurons associated with puberty onset. As a final note, we have used females due to the easy identification of external signs of puberty onset. Further studies in males are necessary to validate the present data in both sexes.

Resource Availability

Lead Contact

Further information and requests for resources and reagents should be directed to and will be fulfilled by the Lead Contact, Carol F. Elias (cfelias@umich.edu).

Materials Availability

This study did not generate new unique reagents.

Data and Code Availability

The original data from all RNA-seq generated in this study are available at Mendeley (www.mendeley.com) under https://data.mendeley.com/datasets/jv988xgnps/1.

METHODS

All methods can be found in the accompanying Transparent Methods supplemental file.

SUPPLEMENTAL INFORMATION

Supplemental Information can be found online at https://doi.org/10.1016/j.isci.2020.101563.

ACKNOWLEDGMENT

This study was funded by grants from the NIH R01HD069702, R03 HD092855 (to C.F.E.), R01 DK056731 (to M.G.M.), and DK 104999 (D.P.O.). X.H. was supported by a fellowship from China Scholarship Council and Sichuan Agricultural University. We acknowledge support from the Bioinformatics Core of the University of Michigan Medical School's Biomedical Research Core Facilities.

AUTHORS CONTRIBUTIONS

X.H. contributed with the conceptualization, investigation, validation, formal analysis, visualization, and writing of original draft; L.L.B. and D.G.-G. contributed with the methodology, supervision of procedures, and review and editing of the original draft; S.S. contributed with methodology and data collection; S.J.A. contributed with methodology and resources; D.P.O. and M.G.M. contributed with resources, review, and editing of the original draft; C.F.E. contributed with the conceptualization, funding acquisition, supervision, validation, visualization, review, and editing of the original draft.

DECLARATION OF INTERESTS

The authors declare no competing interest.

Received: June 18, 2020
Revised: August 16, 2020
Accepted: September 10, 2020
Published: October 23, 2020

REFERENCES

Abreu, A.P., Dauber, A., Macedo, D.B., Noel, S.D., Brito, V.N., Gill, J.C., Cukier, P., Thompson, I.R., Navarro, V.M., Gagliardi, P.C., et al. (2013). Central precocious puberty caused by mutations in the imprinted gene MKRN3. N. Engl. J. Med. *368*, 2467–2475.

Ahima, R.S., Dushay, J., Flier, S.N., Prabakaran, D., and Flier, J.S. (1997). Leptin accelerates the onset of puberty in normal female mice. J. Clin. Invest. *99*, 391–395.

Ahima, R.S., Kelly, J., Elmquist, J.K., and Flier, J.S. (1999). Distinct physiologic and neuronal responses to decreased leptin and mild hyperleptinemia. Endocrinology *140*, 4923–4931.

Ahmed, M.L., Ong, K.K., and Dunger, D.B. (2009). Childhood obesity and the timing of puberty. Trends Endocrinol. Metab. *20*, 237–242.

Allison, M.B., Pan, W., MacKenzie, A., Patterson, C., Shah, K., Barnes, T., Cheng, W., Rupp, A., Olson, D.P., and Myers, M.G., Jr. (2018). Defining the transcriptional targets of leptin reveals a role for Atf3 in leptin action. Diabetes *67*, 1093–1104.

Allison, M.B., Patterson, C.M., Krashes, M.J., Lowell, B.B., Myers, M.G., Jr., and Olson, D.P. (2015). TRAP-seq defines markers for novel populations of hypothalamic and brainstem LepRb neurons. Mol. Metab. *4*, 299–309.

Barash, I.A., Cheung, C.C., Weigle, D.S., Ren, H., Kabigting, E.B., Kuijper, J.L., Clifton, D.K., and Steiner, R.A. (1996). Leptin is a metabolic signal to the reproductive system. Endocrinology *137*, 3144–3147.

Bates, S.H., Stearns, W.H., Dundon, T.A., Schubert, M., Tso, A.W., Wang, Y., Banks, A.S., Lavery, H.J., Haq, A.K., Maratos-Flier, E., et al. (2003). STAT3 signalling is required for leptin regulation of energy balance but not reproduction. Nature *421*, 856–859.

Berkey, C.S., Frazier, A.L., Gardner, J.D., and Colditz, G.A. (1999). Adolescence and Breast Carcinoma Risk (John Wiley & Sons, Inc.), pp. 2400–2409.

Biro, F.M., Khoury, P., and Morrison, J.A. (2006). Influence of obesity on timing of puberty. Int. J. Androl. *29*, 272–277.

Bjornholm, M., Munzberg, H., Leshan, R.L., Villanueva, E.C., Bates, S.H., Louis, G.W., Jones, J.C., Ishida-Takahashi, R., Bjorbaek, C., and Myers, M.G., Jr. (2007). Mice lacking inhibitory leptin receptor signals are lean with normal endocrine function. J. Clin. Invest. *117*, 1354–1360.

Bland, T., Zhu, M., Dillon, C., Sahin, G.S., Rodriguez-Llamas, J.L., Appleyard, S.M., and Wayman, G.A. (2020). Leptin controls glutamatergic synaptogenesis and NMDA-receptor trafficking via fyn kinase regulation of NR2B. Endocrinology *161*, https://doi.org/10.1210/endocr/bqz030.

Burger, L.L., Vanacker, C., Phumsatitpong, C., Wagenmaker, E.R., Wang, L., Olson, D.P., and Moenter, S.M. (2018). Identification of genes enriched in GnRH neurons by translating ribosome affinity purification and RNA-seq in mice. Endocrinology *159*, 1922–1940.

Burt Solorzano, C.M., and McCartney, C.R. (2010). Obesity and the pubertal transition in girls and boys. Reproduction *140*, 399–410.

Campbell, J.N., Macosko, E.Z., Fenselau, H., Pers, T.H., Lyubetskaya, A., Tenen, D., Goldman, M., Verstegen, A.M.J., Resch, J.M., McCarroll, S.A., et al. (2017). A molecular census of arcuate hypothalamus and median eminence cell types. Nat. Neurosci. *20*, 484–496.

Castellano, J.M., Bentsen, A.H., Sánchez-Garrido, M.A., Ruiz-Pino, F., Romero, M., Garcia-Galiano, D., Aguilar, E., Pinilla, L., Diéguez, C., Mikkelsen, J.D., et al. (2011). Early metabolic programming of puberty onset: impact of changes in postnatal feeding and rearing conditions on the timing of puberty and development of the hypothalamic kisspeptin system. Endocrinology *152*, 3396–3408.

Chehab, F.F., Lim, M.E., and Lu, R. (1996). Correction of the sterility defect in homozygous obese female mice by treatment with the human recombinant leptin. Nat. Genet. *12*, 318–320.

Cheng, T.S., Day, F.R., Lakshman, R., and Ong, K.K. (2020). Association of puberty timing with

type 2 diabetes: a systematic review and meta-analysis. PLoS Med. *17*, e1003017.

Clasadonte, J., and Prevot, V. (2018). The special relationship: glia–neuron interactions in the neuroendocrine hypothalamus. Nat. Rev. Endocrinol. *14*, 25–44.

Clement, K., Vaisse, C., Lahlou, N., Cabrol, S., Pelloux, V., Cassuto, D., Gourmelen, M., Dina, C., Chambaz, J., Lacorte, J.M., et al. (1998). A mutation in the human leptin receptor gene causes obesity and pituitary dysfunction [see comments]. Nature *392*, 398–401.

Cohen, P., Zhao, C., Cai, X., Montez, J.M., Rohani, S.C., Feinstein, P., Mombaerts, P., and Friedman, J.M. (2001). Selective deletion of leptin receptor in neurons leads to obesity. J. Clin. Invest. *108*, 1113–1121.

Cottrell, E.C., Campbell, R.E., Han, S.-K., and Herbison, A.E. (2006). Postnatal remodeling of dendritic structure and spine density in gonadotropin-releasing hormone neurons. Endocrinology *147*, 3652–3661.

Cravo, R.M., Frazao, R., Perello, M., Osborne-Lawrence, S., Williams, K.W., Zigman, J.M., Vianna, C., and Elias, C.F. (2013). Leptin signaling in Kiss1 neurons arises after pubertal development. PLoS One *8*, e58698.

Day, F.R., Elks, C.E., Murray, A., Ong, K.K., and Perry, J.R. (2015). Puberty timing associated with diabetes, cardiovascular disease and also diverse health outcomes in men and women: the UK Biobank study. Sci Rep. *5*, 11208.

Day, F.R., Thompson, D.J., Helgason, H., Chasman, D.I., Finucane, H., Sulem, P., Ruth, K.S., Whalen, S., Sarkar, A.K., Albrecht, E., et al. (2017). Genomic analyses identify hundreds of variants associated with age at menarche and support a role for puberty timing in cancer risk. Nat. Genet. *49*, 834.

de Luca, C., Kowalski, T.J., Zhang, Y., Elmquist, J.K., Lee, C., Kilimann, M.W., Ludwig, T., Liu, S.M., and Chua, S.C., Jr. (2005). Complete rescue of obesity, diabetes, and infertility in db/db mice by neuron-specific LEPR-B transgenes. J. Clin. Invest. *115*, 3484–3493.

Donato, J., Jr., Cravo, R.M., Frazao, R., Gautron, L., Scott, M.M., Lachey, J., Castro, I.A., Margatho, L.O., Lee, S., Lee, C., et al. (2011). Leptin's effect on puberty in mice is relayed by the ventral premammillary nucleus and does not require signaling in Kiss1 neurons. J. Clin. Invest. *121*, 355–368.

Egan, O.K., Inglis, M.A., and Anderson, G.M. (2017). Leptin signaling in AgRP neurons modulates puberty onset and adult fertility in mice. J. Neurosci. *37*, 3875–3886.

Elias, C.F., Aschkenasi, C., Lee, C., Kelly, J., Ahima, R.S., Bjorbaek, C., Flier, J.S., Saper, C.B., and Elmquist, J.K. (1999). Leptin differentially regulates NPY and POMC neurons projecting to the lateral hypothalamic area. Neuron *23*, 775–786.

Elias, C.F., and Purohit, D. (2013). Leptin signaling and circuits in puberty and fertility. Cell Mol. Life Sci. *70*, 841–862.

Farooqi, I.S., Matarese, G., Lord, G.M., Keogh, J.M., Lawrence, E., Agwu, C., Sanna, V., Jebb, S.A., Perna, F., Fontana, S., et al. (2002). Beneficial effects of leptin on obesity, T cell hyporesponsiveness, and neuroendocrine/metabolic dysfunction of human congenital leptin deficiency. J. Clin. Invest. *110*, 1093–1103.

Farrow, P., Khodosevich, K., Sapir, Y., Schulmann, A., Aslam, M., Stern-Bach, Y., Monyer, H., and von Engelhardt, J. (2015). Auxiliary subunits of the CKAMP family differentially modulate AMPA receptor properties. Elife *4*, e09693.

Garcia-Galiano, D., Borges, B.C., Donato, J., Jr., Allen, S.J., Bellefontaine, N., Wang, M., Zhao, J.J., Kozloff, K.M., Hill, J.W., and Elias, C.F. (2017). PI3Kalpha inactivation in leptin receptor cells increases leptin sensitivity but disrupts growth and reproduction. JCI Insight *2*, e96728.

Gearing, L.J., Cumming, H.E., Chapman, R., Finkel, A.M., Woodhouse, I.B., Luu, K., Gould, J.A., Forster, S.C., and Hertzog, P.J. (2019). CiiiDER: a tool for predicting and analysing transcription factor binding sites. PLoS One *14*, e0215495.

Han, S.-K., Gottsch, M.L., Lee, K.J., Popa, S.M., Smith, J.T., Jakawich, S.K., Clifton, D.K., Steiner, R.A., and Herbison, A.E. (2005). Activation of gonadotropin-releasing hormone neurons by kisspeptin as a neuroendocrine switch for the onset of puberty. J. Neurosci. *25*, 11349–11356.

Heiman, M., Kulicke, R., Fenster, R.J., Greengard, P., and Heintz, N. (2014). Cell type–specific mRNA purification by translating ribosome affinity purification (TRAP). Nat. Protoc. *9*, 1282.

Henry, F.E., Sugino, K., Tozer, A., Branco, T., and Sternson, S.M. (2015). Cell type-specific transcriptomics of hypothalamic energy-sensing neuron responses to weight-loss. Elife *4*, e09800.

Herman-Giddens, M.E., Slora, E.J., Wasserman, R.C., Bourdony, C.J., Bhapkar, M.V., Koch, G.G., and Hasemeier, C.M. (1997). Secondary sexual characteristics and menses in young girls seen in office practice: a study from the pediatric research in office settings network. Pediatrics *99*, 505–512.

Hou, H., Uuskula-Reimand, L., Makarem, M., Corre, C., Saleh, S., Metcalf, A., Goldenberg, A., Palmert, M.R., and Wilson, M.D. (2017). Gene expression profiling of puberty-associated genes reveals abundant tissue and sex-specific changes across postnatal development. Hum. Mol. Genet. *26*, 3585–3599.

Jackson, T.C., Janesko-Feldman, K., Carlson, S.W., Kotermanski, S.E., and Kochanek, P.M. (2019). Robust RBM3 and β-klotho expression in developing neurons in the human brain. J. Cereb. Blood Flow Metab. *39*, 2355–2367.

Kaplowitz, P.B., Slora, E.J., Wasserman, R.C., Pedlow, S.E., and Herman-Giddens, M.E. (2001). Earlier onset of puberty in girls: relation to increased body mass index and race. Pediatrics *108*, 347–353.

Kennedy, G.C., and Mitra, J. (1963). Body weight and food intake as initiating factors for puberty in the rat. J. Physiol. *166*, 408–418.

Kristensen, P., Judge, M.E., Thim, L., Ribel, U., Christjansen, K.N., Wulff, B.S., Clausen, J.T., Jensen, P.B., Madsen, O.D., Vrang, N., et al. (1998). Hypothalamic CART is a new anorectic peptide regulated by leptin. Nature *393*, 72–76.

Lakshman, R., Forouhi, N., Luben, R., Bingham, S., Khaw, K., Wareham, N., and Ong, K. (2008). Association between age at menarche and risk of diabetes in adults: results from the EPIC-Norfolk cohort study. Diabetologia *51*, 781–786.

Lam, B.Y.H., Cimino, I., Polex-Wolf, J., Nicole Kohnke, S., Rimmington, D., Iyemere, V., Heeley, N., Cossetti, C., Schulte, R., Saraiva, L.R., et al. (2017). Heterogeneity of hypothalamic pro-opiomelanocortin-expressing neurons revealed by single-cell RNA sequencing. Mol. Metab. *6*, 383–392.

Lee, J.M., Kaciroti, N., Appugliese, D., Corwyn, R.F., Bradley, R.H., and Lumeng, J.C. (2010). Body mass index and timing of pubertal initiation in boys. Arch. Pediatr. Adolesc. Med. *164*, 139–144.

Leshan, R.L., Louis, G.W., Jo, Y.-H., Rhodes, C.J., Munzberg, H., and Myers, M.G., Jr. (2009). Direct innervation of GnRH neurons by metabolic- and sexual odorant-sensing leptin receptor neurons in the hypothalamic ventral premammillary nucleus. J. Neurosci. *29*, 3138–3147.

Locke, A.E., Kahali, B., Berndt, S.I., Justice, A.E., Pers, T.H., Day, F.R., Powell, C., Vedantam, S., Buchkovich, M.L., Yang, J., et al. (2015). Genetic studies of body mass index yield new insights for obesity biology. Nature *518*, 197–206.

Maguire, C.A., Song, Y.B., Wu, M., Leon, S., Carroll, R.S., Alreja, M., Kaiser, U.B., and Navarro, V.M. (2017). Tac1 signaling is required for sexual maturation and responsiveness of GnRH neurons to kisspeptin in the male mouse. Endocrinology *158*, 2319–2329.

Mattoo, R.U.H., Sharma, S.K., Priya, S., Finka, A., and Goloubinoff, P. (2013). Hsp110 is a bona fide chaperone using ATP to unfold stable misfolded polypeptides and reciprocally collaborate with Hsp70 to solubilize protein aggregates. J. Biol. Chem. *288*, 21399–21411.

Mizuno, T.M., and Mobbs, C.V. (1999). Hypothalamic agouti-related protein messenger ribonucleic acid is inhibited by leptin and stimulated by fasting. Endocrinology *140*, 814–817.

Morris, D.L., and Rui, L. (2009). Recent advances in understanding leptin signaling and leptin resistance. Am. J. Physiol. Endocrinol. Metab. *297*, E1247–E1259.

Myers, M.G., Cowley, M.A., and Munzberg, H. (2008). Mechanisms of leptin action and leptin resistance. Annu. Rev. Physiol. *70*, 537–556.

Omar, M.H., Kerrisk Campbell, M., Xiao, X., Zhong, Q., Brunken, W.J., Miner, J.H., Greer, C.A., and Koleske, A.J. (2017). CNS neurons deposit laminin alpha5 to stabilize synapses. Cell Rep. *21*, 1281–1292.

Ong, K.K., Ahmed, M.L., and Dunger, D.B. (2006). Lessons from large population studies on timing and tempo of puberty (secular trends and relation to body size): the European trend. Mol. Cell Endocrinol. *254-255*, 8–12.

Ozcan, L., Ergin, A.S., Lu, A., Chung, J., Sarkar, S., Nie, D., Myers, M.G., Jr., and Ozcan, U. (2009).

Endoplasmic reticulum stress plays a central role in development of leptin resistance. Cell Metab. *9*, 35–51.

Padilla, S.L., Qiu, J., Nestor, C.C., Zhang, C., Smith, A.W., Whiddon, B.B., Ronnekleiv, O.K., Kelly, M.J., and Palmiter, R.D. (2017). AgRP to Kiss1 neuron signaling links nutritional state and fertility. Proc. Natl. Acad. Sci. U S A *114*, 2413–2418.

Petridou, E., Syrigou, E., Toupadaki, N., Zavitsanos, X., Willett, W., and Trichopoulos, D. (1996). Determinants of age at menarche as early life predictors of breast cancer risk. Int. J. Cancer *68*, 193–198.

Petry, C.J., Ong, K.K., and Dunger, D.B. (2018). Age at menarche and the future risk of gestational diabetes: a systematic review and dose response meta-analysis. Acta Diabetol. *55*, 1209–1219.

Plant, T.M. (2015). Neuroendocrine control of the onset of puberty. Front. Neuroendocrinol. *38*, 73–88.

Prevot, V., Rio, C., Cho, G.J., Lomniczi, A., Heger, S., Neville, C.M., Rosenthal, N.A., Ojeda, S.R., and Corfas, G. (2003). Normal female sexual development requires neuregulin–erbB receptor signaling in hypothalamic astrocytes. J. Neurosci. *23*, 230–239.

Qu, D., Ludwig, D.S., Gammeltoft, S., Piper, M., Pelleymounter, M.A., Cullen, M.J., Mathes, W.F., Przypek, R., Kanarek, R., and Maratos-Flier, E. (1996). A role for melanin-concentrating hormone in the central regulation of feeding behaviour. Nature *380*, 243–247.

Randi, A.M., Smith, K.E., and Castaman, G. (2018). von Willebrand factor regulation of blood vessel formation. Blood *132*, 132–140.

Rodrigues, B.C., Cavalcante, J.C., and Elias, C.F. (2011). Expression of cocaine- and amphetamine-regulated transcript in the rat forebrain during postnatal development. Neuroscience *195*, 201–214.

Ross, R.A., Leon, S., Madara, J.C., Schafer, D., Fergani, C., Maguire, C.A., Verstegen, A.M., Brengle, E., Kong, D., Herbison, A.E., et al. (2018). PACAP neurons in the ventral premammillary nucleus regulate reproductive function in the female mouse. Elife *7*, e35960.

Rupp, A.C., Allison, M.B., Jones, J.C., Patterson, C.M., Faber, C.L., Bozadjieva, N., Heisler, L.K., Seeley, R.J., Olson, D.P., and Myers, M.G., Jr. (2018). Specific subpopulations of hypothalamic leptin receptor-expressing neurons mediate the effects of early developmental leptin receptor deletion on energy balance. Mol. Metab. *14*, 130–138.

Safe, S., Jin, U.-H., Morpurgo, B., Abudayyeh, A., Singh, M., and Tjalkens, R.B. (2016). Nuclear receptor 4A (NR4A) family - orphans no more. J. Steroid Biochem. Mol. Biol. *157*, 48–60.

Saucedo-Cardenas, O., Quintana-Hau, J.D., Le, W.-D., Smidt, M.P., Cox, J.J., De Mayo, F., Burbach, J.P.H., and Conneely, O.M. (1998). Nurr1 is essential for the induction of the dopaminergic phenotype and the survival of ventral mesencephalic late dopaminergic precursor neurons. Proc. Natl. Acad. Sci. U S A *95*, 4013–4018.

Schwartz, M.W., Erickson, J.C., Baskin, D.G., and Palmiter, R.D. (1998). Effect of fasting and leptin deficiency on hypothalamic neuropeptide Y gene transcription in vivo revealed by expression of a lacZ reporter gene. Endocrinology *139*, 2629–2635.

Schwartz, M.W., Seeley, R.J., Campfield, L.A., Burn, P., and Baskin, D.G. (1996). Identification of targets of leptin action in rat hypothalamus. J. Clin. Invest. *98*, 1101–1106.

Shalitin, S., and Kiess, W. (2017). Putative effects of obesity on linear growth and puberty. Horm Res Paediatr *88*, 101–110.

Simavli, S., Thompson, I.R., Maguire, C.A., Gill, J.C., Carroll, R.S., Wolfe, A., Kaiser, U.B., and Navarro, V.M. (2015). Substance p regulates puberty onset and fertility in the female mouse. Endocrinology *156*, 2313–2322.

Singireddy, A.V., Inglis, M.A., Zuure, W.A., Kim, J.S., and Anderson, G.M. (2013). Neither signal transducer and activator of transcription 3 (STAT3) or STAT5 signaling pathways are required for leptin's effects on fertility in mice. Endocrinology *154*, 2434–2445.

Sisk, C.L., and Foster, D.L. (2004). The neural basis of puberty and adolescence. Nat. Neurosci. *7*, 1040–1047.

Terasawa, E., and Fernandez, D.L. (2001). Neurobiological mechanisms of the onset of puberty in primates. Endocr. Rev. *22*, 111–151.

Topaloglu, A.K. (2017). Update on the genetics of idiopathic hypogonadotropic hypogonadism. J. Clin. Res. Pediatr. Endocrinol. *9*, 113–122.

True, C., Verma, S., Grove, K.L., and Smith, M.S. (2013). Cocaine- and amphetamine-regulated transcript is a potent stimulator of GnRH and kisspeptin cells and may contribute to negative energy balance-induced reproductive inhibition in females. Endocrinology *154*, 2821–2832.

Walvoord, E.C. (2010). The timing of puberty: is it changing? Does it matter? J. Adolesc. Health *47*, 433–439.

Williams, K.W., Sohn, J.W., Donato, J., Jr., Lee, C.E., Zhao, J.J., Elmquist, J.K., and Elias, C.F. (2011). The acute effects of leptin require PI3K signaling in the hypothalamic ventral premammillary nucleus. J. Neurosci. *31*, 13147–13156.

Wójcik-Gładysz, A., and Polkowska, J. (2006). Neuropeptide Y–a neuromodulatory link between nutrition and reproduction at the central nervous system level. Reprod. Biol. *6*, 21–28.

Wood, C.L., Lane, L.C., and Cheetham, T. (2019). Puberty: normal physiology (brief overview). Best Pract. Res. Clin. Endocrinol. Metab. *33*, 101265.

Yamamoto, K., de Waard, V., Fearns, C., and Loskutoff, D.J. (1998). Tissue distribution and regulation of murine von Willebrand factor gene expression in vivo. Blood *92*, 2791–2801.

Yang, L., Li, P., Fu, S., Calay, E.S., and Hotamisligil, G.S. (2010). Defective hepatic autophagy in obesity promotes ER stress and causes insulin resistance. Cell Metab *11*, 467–478.

Yao, J., Guihard, P.J., Blazquez-Medela, A.M., Guo, Y., Liu, T., Boström, K.I., and Yao, Y. (2016). Matrix Gla protein regulates differentiation of endothelial cells derived from mouse embryonic stem cells. Angiogenesis *19*, 1–7.

Yura, S., Ogawa, Y., Sagawa, N., Masuzaki, H., Itoh, H., Ebihara, K., Aizawa-Abe, M., Fujii, S., and Nakao, K. (2000). Accelerated puberty and late-onset hypothalamic hypogonadism in female transgenic skinny mice overexpressing leptin. J. Clin. Invest. *105*, 749–755.

Zeisel, A., Hochgerner, H., Lönnerberg, P., Johnsson, A., Memic, F., van der Zwan, J., Häring, M., Braun, E., Borm, L.E., La Manno, G., et al. (2018). Molecular architecture of the mouse nervous system. Cell *174*, 999–1014.e1022.

Zetterström, R.H., Solomin, L., Jansson, L., Hoffer, B.J., Olson, L., and Perlmann, T. (1997). Dopamine neuron agenesis in nurr1-deficient mice. Science *276*, 248–250.

Zhu, Z., and Reiser, G. (2018). The small heat shock proteins, especially HspB4 and HspB5 are promising protectants in neurodegenerative diseases. Neurochem. Int. *115*, 69–79.

Zuure, W.A., Roberts, A.L., Quennell, J.H., and Anderson, G.M. (2013). Leptin signaling in GABA neurons, but not glutamate neurons, is required for reproductive function. J. Neurosci. *33*, 17874–17883.

iScience, Volume *23*

Supplemental Information

Hypothalamic and Cell-Specific Transcriptomes Unravel a Dynamic Neuropil Remodeling in Leptin-Induced and Typical Pubertal Transition in Female Mice

Xingfa Han, Laura L. Burger, David Garcia-Galiano, Seokmin Sim, Susan J. Allen, David P. Olson, Martin G. Myers Jr., and Carol F. Elias

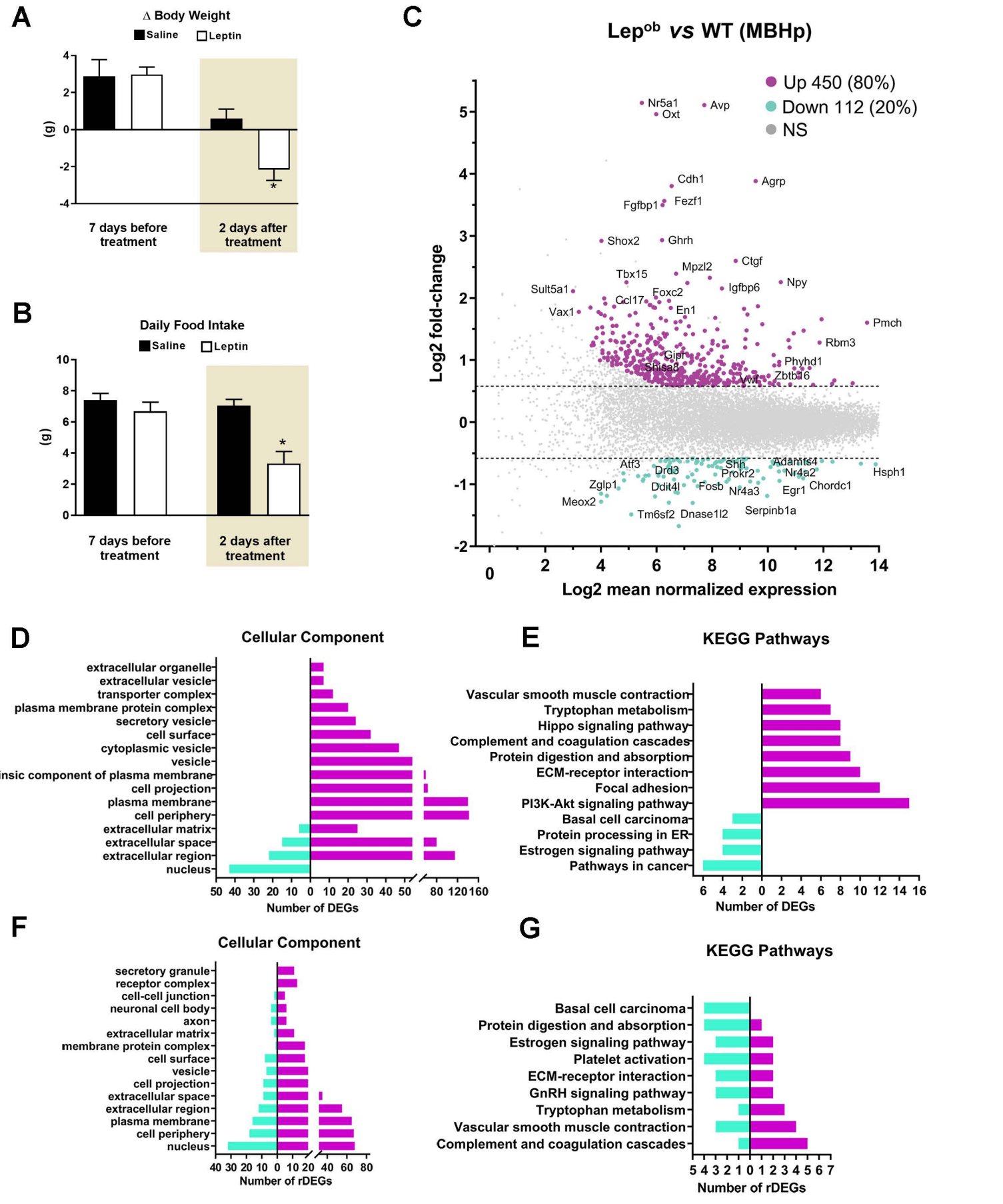

Figure S1. Related to Figure 1. (A-B) Changes in body weight and food intake of leptin-deficient Lep^{ob} mice before and after treatment with saline or leptin. Mice with clear vaginal opening were euthanized. (C) Differentially expressed genes (DEGs) in the posterior mediobasal hypothalamus (MBHp) between Lep^{ob} and WT female mice. GO (example of cellular compartment) and KEGG pathways of DEGs (D-E) and rDEGs (F-G) in the MBHp comparing Lep^{ob} vs WT (D-E) and Lep^{ob} vs Lep^{ob} + leptin (F-G). Purple, upregulated; Green, downregulated; NS, non significant.*p<0.05 by Student t test. Data presented as mean +/- SEM.

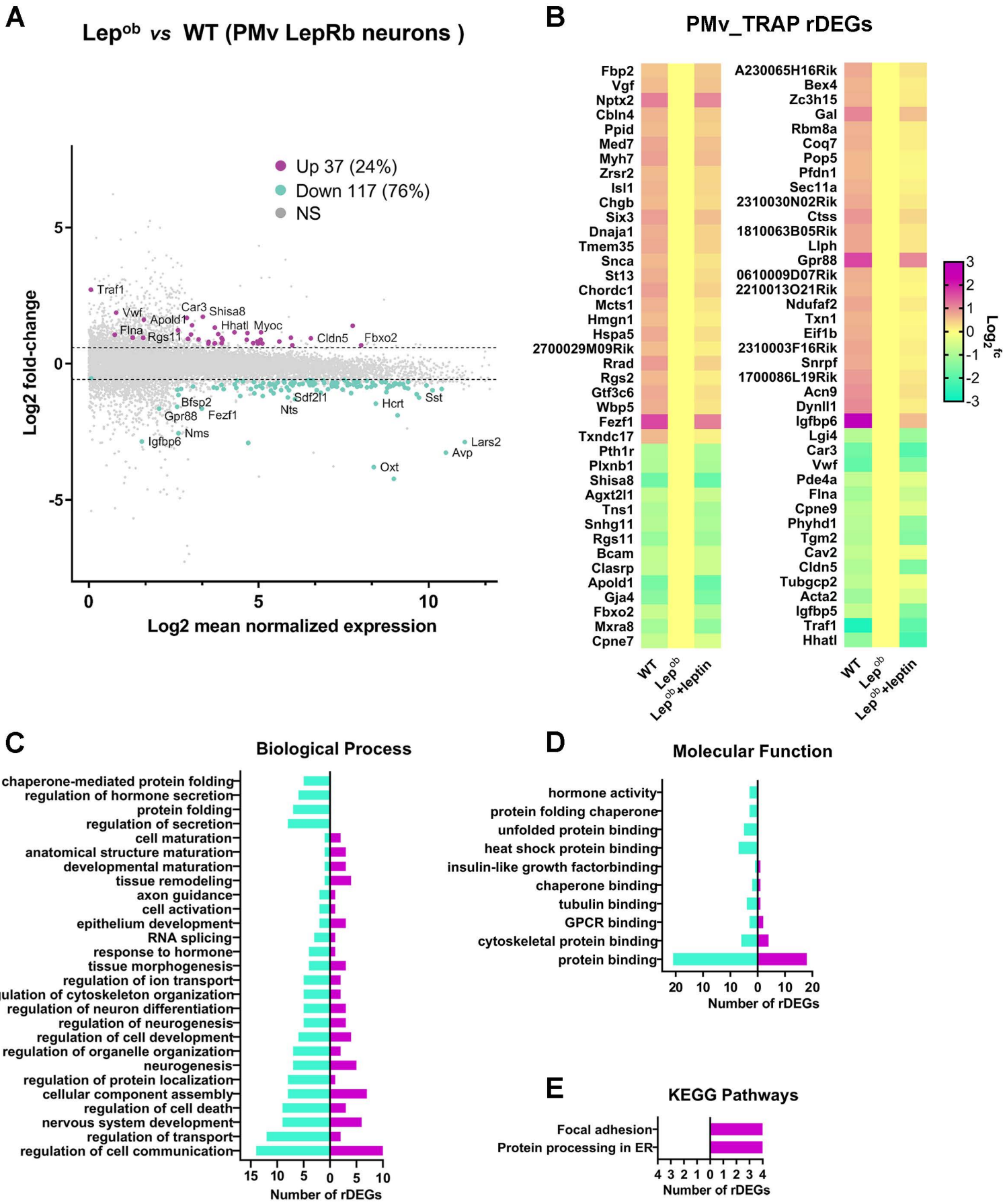

Figure S2. Related to Figure 2. Differentially expressed genes (TRAP_DEGs) in LepRb PMv neurons comparing Lep^{ob} and WT mice. (A) Most of the DEGs were downregulated in Lep^{ob} females. (B) recovered DEGs (rDEGs) enriched in PMv LepRb neurons. (C-E) GO and KEGG pathways associated with rDEGs. Purple, upregulated; Green, downregulated; NS, non-significant.

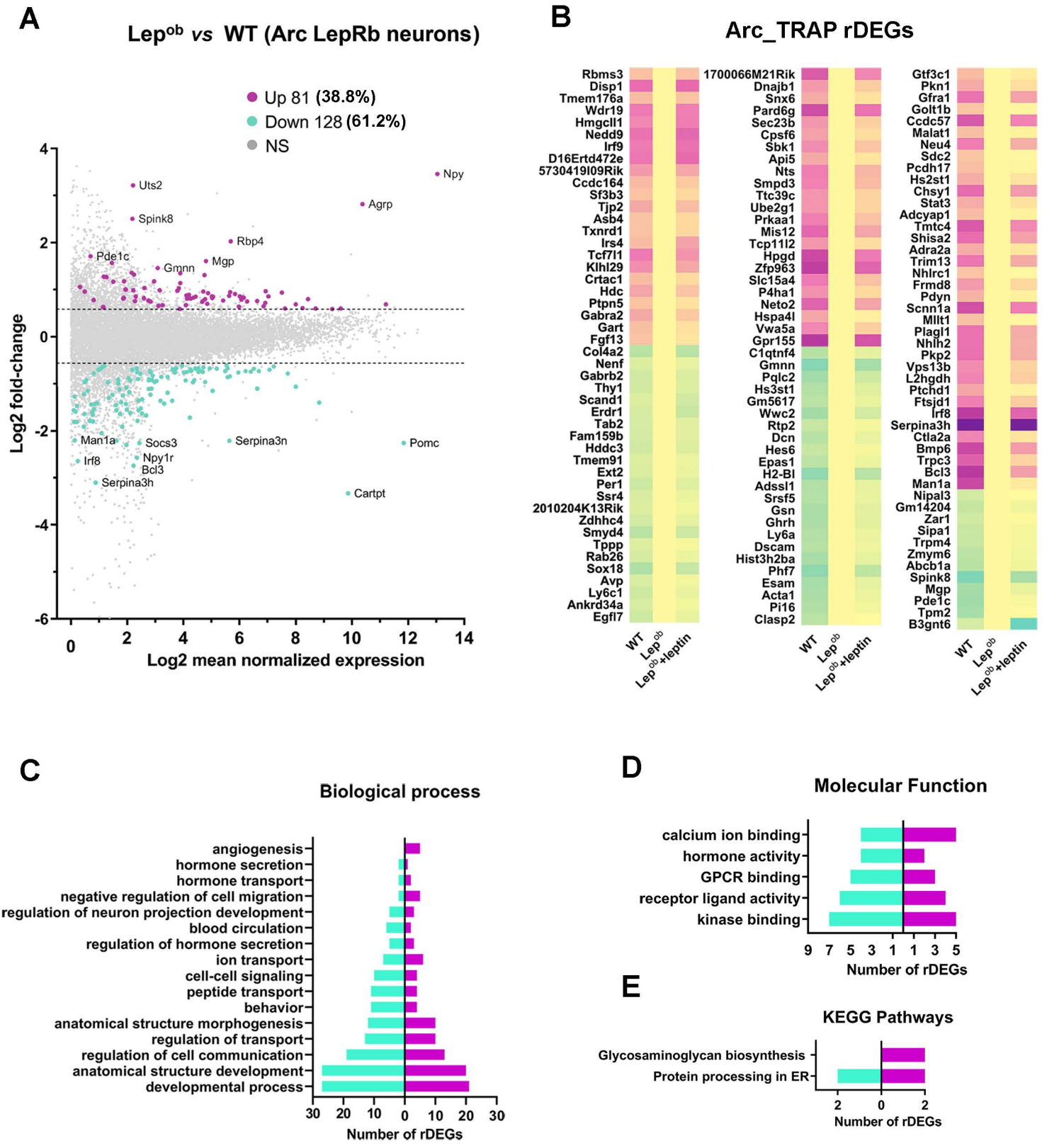

Figure S3. Related to Figure 2. Differentially expressed TRAP genes (TRAP_DEGs) in LepRb Arc neurons comparing Lep^{ob} and WT. (A) Most of these TRAP DEGs were downregulated in Lep^{ob} females. (B) recovered DEGs (rDEGs) after short-term leptin treatment. (C-E) GO and KEGG pathways associated with rDEGs. Purple, upregulated; Green, downregulated; NS, non significant.

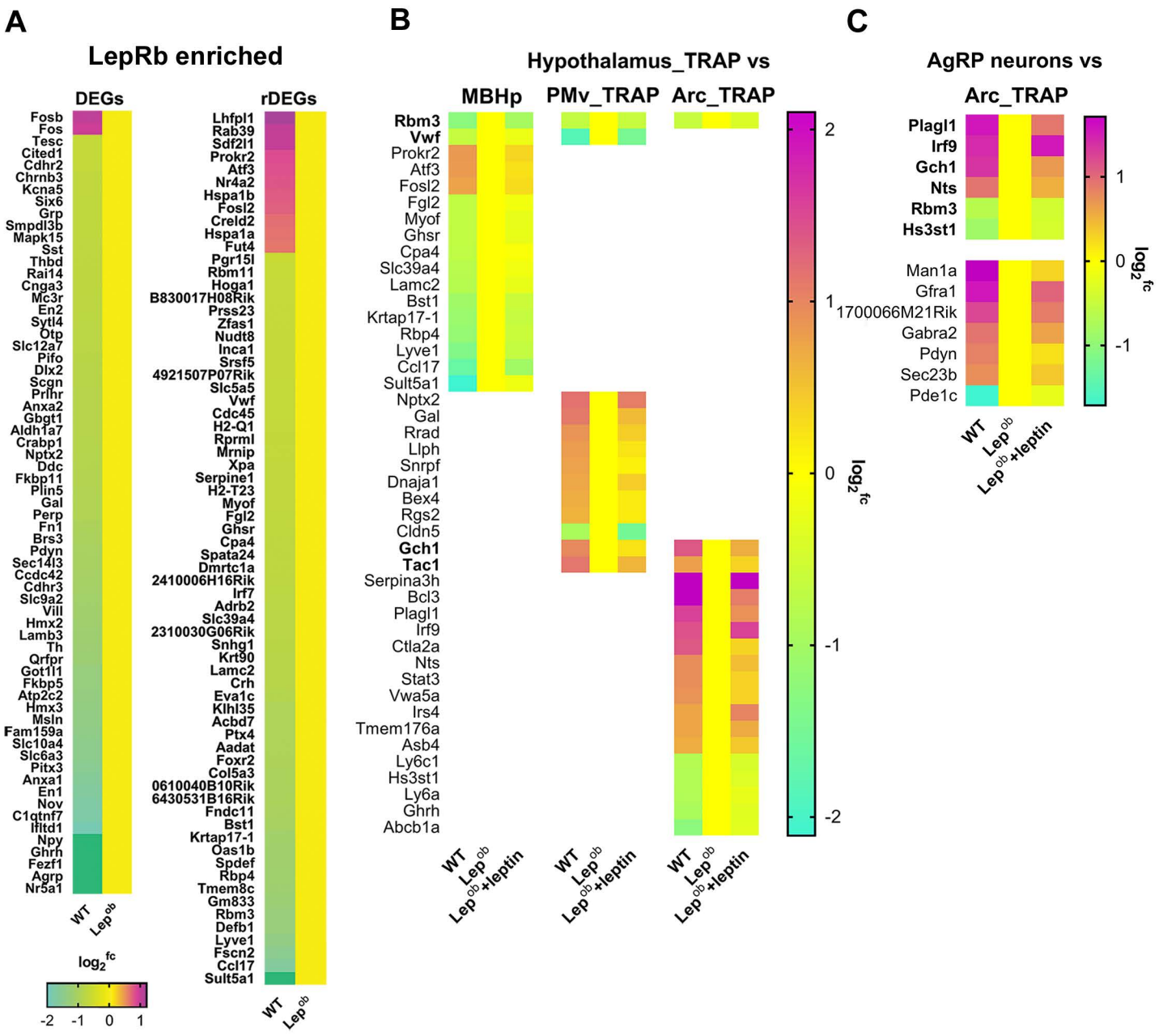

Figure S4. Related to Figure 2. Overlapping analysis using published database for further validation. A, B, comparative analysis of MBHp, PMv LepRb TRAP-seq, Arc LepRb TRAP-seq and TRAP DEGs obtained from hypothalamic blocks (Allison et al., 2015 and 2018). Only LepRb enriched and leptin regulated DEGs were used. C, Comparative analysis between Arc LepRb TRAP-seq and DEGs in AgRP neurons following nutritional challenges (Henry et al., 2015).

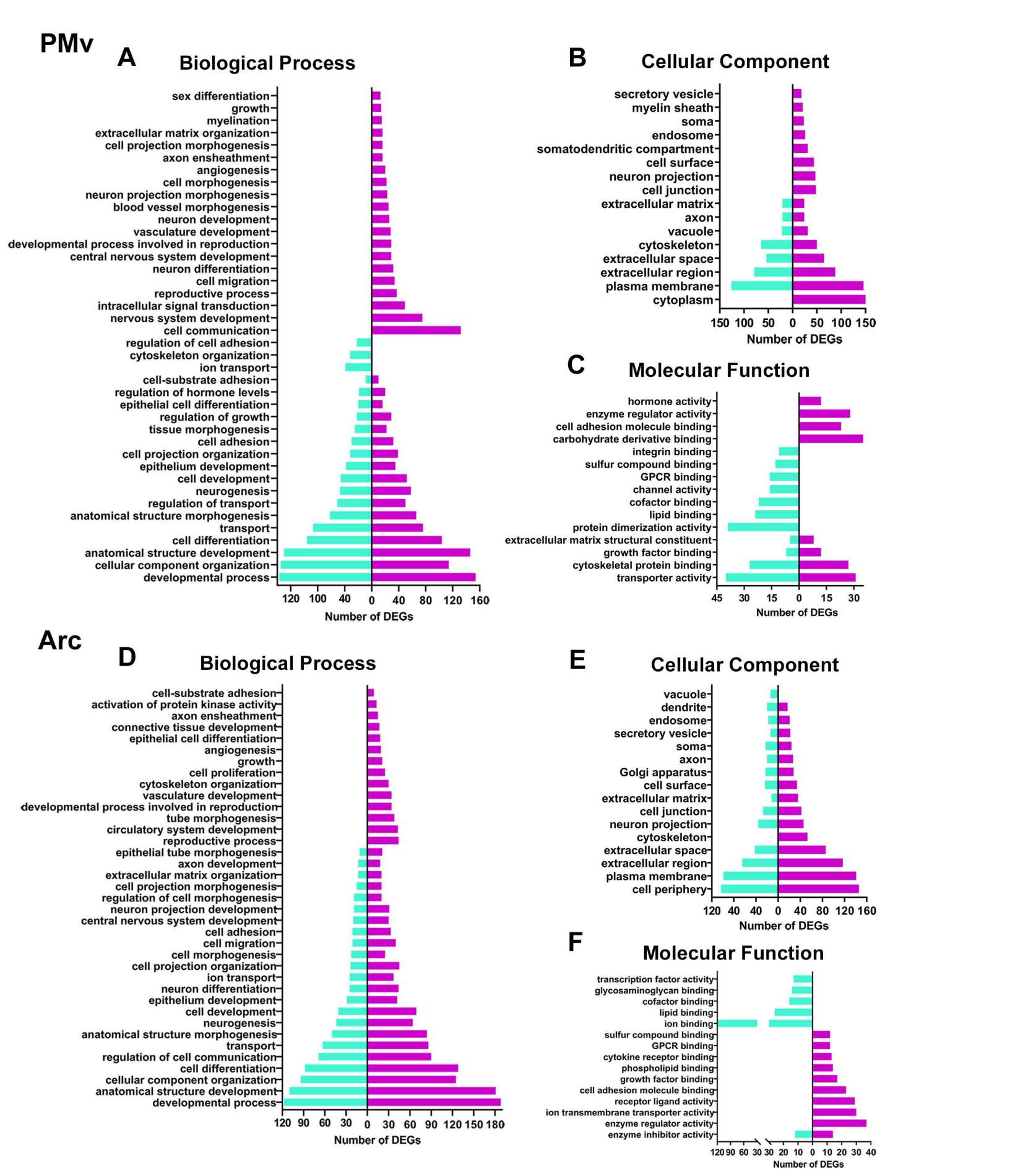

Figure S5. Related to Figure 3. Categorization of differentially expressed genes (DEGs) in the ventral premammillary nucleus (PMv, A-C) and arcuate nucleus (Arc, D-F) of prepubertal vs diestrous females.

Table S5: Primers used in qPCR.

Genes	Primer sequence (5'-3')	Product length (bp)
18s	F: TGACTCAACACGGGAAACC R: AACCAGACAAATCGCTCCAC	125
Ccl17	F: GCTGGTATAAGACCTCAGTGGAGTGT R: CAATCTGATGGCCTTCTTCACA	116
Cd46	F: ATGCCTGTGAACTACCACGGCCATTTGAAG R: TTTGCCAAATGAAGGGTCTTG	230
Crh	F: TCTGCAGAGGCAGCAGTGCGGG R: CGGATCCCCTGCTGAGCAGGGC	150
Gipr	F: CTGCCTGCCGCACGGCCCAGAT R: GCGAGCCAGCCTCAGCCGGTAA	383
Lhx9	F: CGTCTCTACGCTTCTGCATC R: GGCGGAAAGGACACGAAT	135
Meox2	F: TGGCAGCAAAAGGAAAAGCG R: GGAACCACACTTTCACCTGTCT	218
Nanos2	F: ATTCAGAGCCGGAAGCAAAG R: GACTGCTGTTGAGTGGACAA	285
Nr4a2	F: TTCCACCAGAACTACGTGGC R: CAGCTAGACACAGGAGTGCC	116
Pdlim3	F: TTGACAGGGCAGAAACTCGC R: GAAGCGCTCACTACCTGTCT	187
Pla2g3	F: GGGAACTCTGCTGAAAATGC R: AATGGTTTGTGGGCACTGAT	90
Rbp4	F: GACAAGGCTCGTTTCTCTGG R: AAAGGAGGCTACACCCCAGT	243
Shh	F: AGCAGACCGGCTGATGACTC R: TCACTCCAGGCCACTGGTTC	83
Shox2	F: TGGAACAACTCAACGAGCTGGAGA R: TTCAAACTGGCTAGCGGCTCCTAT	200
Wnt7a	F: GGCTACAACACACACCAGTAT R: GATCTGACCTGTGACCTCATTC	137
Zbtb16	F: CCTGGACAGTTTGCGACTGA R: TCCGTGCCAGTATGGGTCT	138
Zglp1	F: GGTTCAAGGGGGTAACTCTGG R: AGCAACTGGAACAACGGGTG	282

Note: F, Forward primer; R, Reverse primer

Transparent Methods

Key Resources Table

REAGENT or RESOURCE	SOURCE	IDENTIFIER
Antibodies		
Sheep anti-VWF antibody	Abcam Cat#ab11713	RRID:AB_298501
Rabbit anti-Laminin antibody	Novus Cat#NB300-144	RRID:AB_10001146
Rabbit anti-CART antibody	Phoenix Cat#H-003-62	RRID:AB_2313614
Goat anti-Rabbit IgG (H+L) Highly Cross-Adsorbed Secondary Antibody, Alexa Fluor Plus 488	Invitrogen Cat#A32731	RRID:AB_2633280
Donkey anti-Rabbit IgG (H+L) Highly Cross-Adsorbed Secondary Antibody, Alexa Fluor Plus 488	Invitrogen Cat#A32790	RRID:AB_2762833
Donkey anti-Sheep IgG (H+L) Cross-Adsorbed Secondary Antibody, Alexa Fluor 594	Invitrogen Cat#A-11016	RRID:AB_2534083
Chemicals, Peptides, and Recombinant Proteins		
Biotin-Protein L	GeneScript	Cat#M00097
BSA	Jackson Immuno Research	Cat#0001-000-162
Cycloheximide (CHX)	Sigma	Cat#C7698
Dithiothreitol Molecular Biology Reagent	Sigma	Cat#D9779
D-(+)-Glucose Bioxtra	Sigma	Cat#G7528
DHPC	Avanti Polar Lipids/VWR	Cat#100122-252
EDTA Free, Protease Cocktail Tablets	Roche	Cat#11836170001
GFP Ab, C8	Memorial-Sloan Kettering Monoclonal Antibody Facility	Cat#HTZ-GFP-19C8
GFP Ab, F7	Memorial-Sloan Kettering Monoclonal Antibody Facility	Cat#HTZ-GFP-19F7
HBSS, Hank'S balanced salt solution, 10X	Invitrogen/Life Technologies	Cat#14065-056
HEPES,1M	Affymetrix/Fisher	Cat#16924
iTaq™ Universal SYBR® Green Supermix	BIO-RAD	Cat#1725120
KCl, 2M	Applied Biosystems/Life Technologies	Cat#AM9640G
Leptin	A.F. Parlow, NHPP, Harbor-UCLA Medical Center, Torrance, California, USA	N/A
Methanol, Anhydrous, 99.8%	Sigma	Cat#322415
MgCl2, 1M	Applied Biosystems/Life Tech	Cat#AM9530G

NP-40, 10% Sterile, Rnase Free Vials	AG Scientific	Cat#P1505
PBS, 10X	Applied Biosystems/Life Tech	Cat#AM9625
QIAzol Lysis Reagent	Qiagen	Cat#79306
RNAsin	Promega/Fisher	Cat#N2515
RNAse Free Water	Applied Biosystems/Life Tech	Cat#AM9937
Roche Protector Rnase Inhibitor	Roche/Sigma	Cat#3335402001
Sodium Azide, 99.5%	Sigma	Cat#S2002
Sodium Bicarbonate Bioxtra	Sigma	Cat#S6297
Steptavidin T1 Dynabeads	Invitrogen/Life Technologies	Cat#65601
Superasin	Applied Biosystems/Life Tech	Cat#AM2694
Critical Commercial Assays		
DNAse I	Sigma-Aldrich	Cat#AMPD1
miRNeasy®mini Kit	Qiagen	Cat# 217004
Illumina TruSeq mRNA Sample Preparation v2 kit	Illumina	Catalog #s RS-122-2001, RS-122-2002
KAPA Library Quantification Kits	Kapa Biosystems	Cat# KK4835
RNeasy Micro Kit	Qiagen	Cat#74004
SMARTer Ultra Low RNA Kit for Illumina Sequencing	Clontech	Cat#634936
SuperScript™ II	Invitrogen	Cat#18064022
Deposited Data		
Sequencing data listed in the Tables	This paper	Table S1-4
Experimental Models: Organisms/Strains		
C57BL/6J mice	Jackson labs	Stock # 000664
$Lep^{ob/+}$ mice	Jackson labs	Stock # 000632
$LepR^{cre}$ mice	Leshan et al., 2006	N/A
$Rosa^{eGFP\text{-}L10a/eGFP\text{-}L10a}$ mice	Krashes et al., 2014	N/A
Oligonucleotides		
Primers for qPCR quantification	This paper	See Table S5
Software and Algorithms		
CiiiDER	Gearing et al., 2019	http://ciiider.com/
Cytoscape(v3.7.2)	Cytoscape Software	http://www.cytoscape.org/
Cufflinks/Cuffdiff(2.1.1)	Trapnell et al., 2012	http://cole-trapnell-lab.github.io/cufflinks/install/
DAVID(v6.8)	Huang da et al., 2009	https://david.ncifcrf.gov/
GraphPad Prism (v8.0)	GraphPad Software	https://www.graphpad.com/

R (v 3.6.1)	R Software	https://www.R-project.org/
STRING (v11.0)	String Consortium	https://string-db.org/cgi/input.pl
TopHat (v2.0.13)	Trapnell et al., 2012	http://ccb.jhu.edu/software/tophat/downloads/
VLAD (v1.8.0)	Richardson & Bult, 2015	http://proto.informatics.jax.org/prototypes/vlad/

Experimental Model and Subject Details

Mice

$Lep^{ob/+}$ mouse (ob/+; JAX® mice, stock # 000632) purchased from Jackson labs were intercrossed to generate $Lep^{+/+}$ (WT) and $Lep^{ob/ob}$ (Lep^{ob}) female littermates. $Lep^{ob/+}$ mice were crossed to $LepR^{cre}$ (Leshan et al., 2006) to obtain $Lep^{ob/+}LepR^{cre}$ mice, which were subsequently crossed to $Rosa^{eGFP\text{-}L10a/eGFP\text{-}L10a}$ mice (Allison et al., 2015; Krashes et al., 2014) to generate $Lep^{ob/+}LepRb^{cre}Rosa^{eGFP\text{-}L10a}$ (LepRbLepR$^{eGFP\text{-}L10a}$) mice, which express GFP-labeled L10a ribosomal protein targeted to LepRb neurons. $Lep^{ob/+}LepRb^{cre}Rosa^{eGFP\text{-}L10a}$ mice were then intercrossed to generate $Lep^{+/+}$; $LepRb^{cre/cre}Rosa^{eGFP\text{-}L10a/eGFP\text{-}L10a}$ and $Lep^{ob/ob}LepRb^{cre/cre}Rosa^{eGFP\text{-}L10a/eGFP\text{-}L10a}$ ($LepRb^{eGFP\text{-}L10a}$) female littermates. Adult (PND60-70) and prepubertal (PND18) C57BL/6J females were generated from the intercrossing of C57BL/6J mice (JAX® mice, stock # 000664). Mice were bred at the University of Michigan and maintained in a light- (12 h light/dark cycle) and temperature- (21 to 23°C) controlled environment with free access to water and food. Mice were fed with a phytoestrogen-reduced diet 2016 (16% protein/4% fat, Teklad 2916 irradiated global rodent diet, Envigo) to minimize the effect of exogenous estrogen in pubertal development. All procedures involving mice were approved by the University of Michigan IACUC in accordance with AAALAC and NIH guidelines (protocol # PRO08712).

Methods

Leptin treatment and harvesting of MBHp

Mice (PND60-70) were divided into three groups (n=4/group): a) wildtype (WT) diestrous females treated with intraperitoneal (ip.) saline; b) leptin-deficient (Lep^{ob}) females treated with ip. saline (ob); and c) Lep^{ob} females treated with ip. leptin (Lep^{ob}+leptin) 2.5 μg/g for 2 days, at 9:00 AM and 5:00 PM (leptin from A.F. Parlow, Harbor-UCLA Medical Center, National Hormone and Peptide Program). One hour after the last saline or leptin injection (at 10:00 AM), females were euthanized by decapitation following anesthesia (isoflurane) and brains were harvested. Frontal sections of the hypothalamus (1 mm-thick) were collected using a brain matrix (Ted Pella, Inc. cat# 15003). The MBHp was micro-dissected, processed for RNA extraction and submitted for RNAseq analysis.

Translating Ribosome Affinity Purification (TRAP) of PMv and Arc LepRb cells

Diestrous $LepR^{eGFP\text{-}L10a}$ and $Lep^{ob}LepR^{eGFP\text{-}L10a}$ female mice (PND60-70) were used. The expression of eGFP-L10a in LepRb neurons in the hypothalamus of the $LepR^{eGFP\text{-}L10a}$ mouse line has been verified and validated by our group (Allison et al., 2018; Allison et al., 2015).The experimental design and saline/leptin treatment were the same as detailed in the previous item ("Leptin treatment and harvesting of MBHp"). The PMv and Arc were collected separately from the left and right sides of each individual mouse brain by micro punches (1.25 mm diameter). The third ventricle was used as anatomical reference for the medial and dorsal borders of the hypothalamus and the fornix was used as the lateral limit of the medial hypothalamus. Preliminary experiments assessing RNA concentration determined the need to pool micro punches from both sides of three mice per treatment group. Each pooled set of PMv or Arc punches was considered a single biological replicate, and four biological replicates in each treatment group were used. The mRNA was isolated from eGFP-tagged ribosomes, as well as eGFP-depleted supernatant (Allison et al., 2015; Burger et al., 2018; Heiman et al., 2014). Tissue punches were immediately homogenized in ice-cold lysis buffer [20 mM HEPES-KOH, 150 mM KCl, and 10 mM $MgCl_2$ (Affymetrix/Thermo Fisher Scientific); 1× EDTA Free Protease Inhibitor and 1.25% volume-to-volume ratio (v/v) of RNAse Inhibitor (Roche, Indianapolis, IN), 0.625% v/v RNAsin (Promega, Madison, WI), 0.625% v/v Superasin (Invitrogen/Thermo Fisher Scientific), 0.5 mM dithiothreitol and 0.1 mg/ml cycloheximide. Lysis buffer volume was adjusted for input amounts of PMv and Arc punches (100 µL of lysis buffer per punches). Anti-GFP (HtzGFP-19F7 and HtzGFP-19C8; Antibody and Bioresource Core Facility, Memorial Sloan Kettering Cancer Center, New York, NY)-coated streptavidin magnetic beads (Streptavidin T1 Dynabeads; Invitrogen/Thermo Fisher Scientific) were applied to the samples. Immunoprecipitation occurred overnight at 4°C. Polysome-RNA complexes bound to the anti–GFP-coated streptavidin magnetic beads (LepRb neuron specific) were separated from the supernatant by a magnet; RNA was isolated using the RNeasy Micro Kit with on-column DNAsin (Qiagen, Valencia, CA). The RNA samples were subjected to RNA quantification and quality evaluation using the RNA 6000 Pico Chip (Agilent Technologies) for RNAseq. Before generating cDNA libraries, LepRb-enhanced and LepRb-depleted RNAs were reverse transcribed (Allison et al., 2018; Allison et al., 2015; Burger et al., 2018) and amplified for *Lepr* and *Actb* (β-actin, reference gene) using Taqman qPCR to determine enrichment for *Lepr*. The *Lepr* expression levels were normalized to *Actb* (no difference between groups), and enrichment was calculated as relative expression in LepRb-enhanced RNA samples divided by the normalized relative expression in the LepRb-depleted samples. The LepRb-enhanced RNA of each sample was used to create cDNA libraries with the SMARTer v4 Ultra Low Kit and Low Input DNA library Pre Kits (Clontech) (Burger et al., 2018).

Tissue harvesting in prepubertal vs diestrus females

C57BL/6J prepubertal (P18) and adult diestrous (P60-70) females (n=4 per group) were euthanized under isoflurane anesthesia. Vaginal cytology was monitored for approximately 7 days before tissue collection in adult females to determine estrous cycle stage. Only normally cycling females were used. After euthanasia, uterine weight was measured to confirm diestrus (< 100 mg). PMv and Arc micro punches were dissected and collected as detailed in the

previous section (“Translating Ribosome Affinity Purification (TRAP) of PMv and Arc LepRb cells”) and processed for RNAseq analysis.

RNA-sequencing and Data Processing

RNA was extracted with miRNeasy®mini Kit (Qiagen, cat# 217004) according to the manufacturer protocol. RNA was assessed for quality using the TapeStation (Agilent, Santa Clara, CA). Samples with RNA integrity numbers (RINs) of 8 or greater were subjected to Illumina TruSeq mRNA Sample Preparation v2 kit (Catalog #s RS-122-2001, RS-122-2002), and 1-3g of total RNA was purified to mRNA using polyA purification. The mRNA was fragmented via chemical fragmentation and reverse transcribed into cDNA using reverse transcriptase and random primers. The 3’ ends of the cDNA were adenylated, and 6-nucleotide-barcoded adapters ligated. The products were purified and enriched by PCR to generate the final cDNA library. Final libraries were checked for quality and quantity by TapeStation (Agilent) and qPCR using Kapa's library quantification kit for Illumina Sequencing platforms (Kapa Biosystems, cat# KK4835). They were clustered on the cBot (Illumina) and 4 samples per lane were sequenced on a 50-cycle single end run in a HiSeq 2500 (Illumina) by the University of Michigan DNA Sequencing and Bioinformatics Cores. The Tuxedo Suite software package was used for alignment, differential expression analysis, and post-analysis diagnostics (Trapnell et al., 2013). Cufflinks/CuffDiff (http://coletrapnell-lab.github.io/cufflinks/) (Trapnell et al., 2012) was used for quantitation, normalization, and determination of differential expression using University of California Santa Cruz (Santa Cruz, CA) mm10.fa as the reference genome sequence (http:// genome.ucsc.edu/). Hierarchical cluster analysis was conducted to assemble genes with similar expression patterns across groups using Cluster 3.0 software. After normalization of the expression of each gene by log2 transformation, gene clustering was performed with average linkage method with Euclidean distance. The hierarchical cluster heatmap was organized by Java TreeView software. DEGs in pairwise comparisons among groups were determined using Cufflinks/Cuffdiff analysis, with thresholds for differential expression set to fold change (fc)>1.5 or <0.66 and a false discovery rate (q value) of ≤ 0.05. The Gene List analysis and Visualization (VLAD) v1.8.0 was used to define the enriched biological processes (BP), cellular component (CC) and molecular function (MF) of DEGs. For pathway analysis, the Kyoto Encyclopedia of Genes and Genomes (KEGG) pathway database using DAVID v6.8 was used to reveal physical and/or functional interactions among the genes. Gene ontology (GO) and pathway terms showing unadjusted p-values < 0.05 were selected. STRING online database (http://string-db.org) was used to assess protein-protein interaction (PPI) and Cytoscape software (http://www.cytoscape.org/) was employed to visualize PPI network interaction of common DEGs.

Mapping of phosphoSTAT binding sites

The potential pSTAT3/STAT5 binding sites across the promoter region (1500bp upstream and 500bp downstream of the transcription start site) of the core genes were scanned by CiiiDER software. JASPAR2020_CORE_vertebrates clustering was used as the transcription factor position frequency matrix. Deficit threshold was defined as 0.15. One thousand genes with close to zero-fold change between WT and Lep^{ob} from PMv TRAP-seq and Arc TRAP-seq, respectively, were used as the background gene list to identify significantly over-represented

STAT3/STAT5-targeting core genes in PMv and Arc, respectively. Fisher's exact test was used and gene coverage p-value < 0.05 was considered significant.

Analysis of Overlapping DEGs in all three RNAseq Assays

All analyses were generated in R (v3.6.1) language for statistical computing (https://www.R-project.org/). Independent RNA-seq data (MBHp, TRAPseq, and PP vs Di CuffDiff results) and DAVID enrichments were used as input files (Huang da et al., 2009a, b; Trapnell et al., 2012). To determine shared DAVID functional enrichments between comparisons from different projects, shared DEGs and identity of all measured genes across the comparisons were first determined. Group comparisons:

Group 1: WT_v_Ob_Saline_DE.xlsx (MBHp), PMV.diestrus_v_PMV.ob_saline.xlsx (TRAPseq), PMV.Adult_v_PMV.Pre.xlsx (PP vs Di);

Group 2: WT_v_Ob_Saline_DE.xlsx (MBHp), ARC.diestrus_v_ARC.ob_saline.xlsx (TRAPseq), ARC.Adult_v_ARC.Pre.xlsx (PP vs Di);

Group 3: Supp Table 1 DEGs (MBHp), Supp Table 4 PMV DEGs (TRAPseq), PMV.Adult_v_PMV.Pre.xlsx (PP vs Di);

Group 4: Supp Table 1 DEGs (MBHp), Supp Table 6 Arc DEGs (TRAPseq), ARC.Adult_v_ARC.Pre.xlsx (PP vs Di)

Shared DEGs and all measured genes between comparison sets were converted from gene symbols to ENSEMBL ids and used as query sets and background sets, respectively, for DAVID enrichments using R package RDAVIDWebService (v3.10) (Fresno and Fernandez, 2013). Enrichments were repeated with rDEGs as query sets for Group 3 and Group 4. The background sets generated for Group 1 (PMv) and Group 2 (Arc) were used for DEGs and rDEG DAVID enrichments for Group 3 (PMv) and Group 4 (Arc), matched by cell-type.

Quantitative PCR (qPCR) validation of RNA-sequencing data

To validate the RNAseq data, PMv and Arc samples obtained by micro punches were evaluated. Tissue was homogenized in Qiazol reagent (Qiagen), and total RNA was isolated using an RNA extraction kit (miRNeasy, Qiagen). Total RNA (200 ng) was used to synthesize cDNA using SuperScript II reverse transcriptase and random primers (Invitrogen) according to the manufacturer's protocol. Gene expression analyses were performed by qPCR using a CFX-384 Bio-Rad Real-Time PCR detection system (SYBR Green reaction).The mRNA levels were normalized to the *18s* ribosomal RNA reference gene, and changes related to the control levels (WT, diestrous females) were determined using $2^{-\Delta\Delta Ct}$ method. We initially evaluated the variation of *18s* Ct values across samples and experiment groups and no difference was observed (all groups showed Ct values ranging from 12.8 to 13.4) indicating the *18s* was an adequate reference gene. Primers for targeted and reference genes are listed in Table S5.

Immunofluorescence

A group of PP and Di mice were intracardially perfused with 10% formalin, and brains were prepared for histological examination. Hypothalamic sections of PP and Di females were labeled with sheep anti-VWF (1:1,000 Abcam, cat#ab11713) and/or rabbit anti-Laminin (1:1000 Novus, cat#NB300-144). According to the manufacturers, the laminin antibody is pan-specific and

reacts with all laminin isoforms tested: Laminin-1 (alpha-1, beta-1, and gamma-1) and Laminin-2 (alpha-2, beta-1, and gamma-1). Following overnight incubation at room temperature, tissue was incubated in secondary conjugated to AF488 or AF594 (Invitrogen) for 1h. Another series of hypothalamic sections from PP and Di mice were also incubated in rabbit anti-CART peptide (1:10,000 Phoenix, cat#H-003-62) and processed for immunoperoxidase using DAB and silver enhancement.

QUANTIFICATION AND STATISTICAL ANALYSIS

Data other than RNAseq are reported as mean ± standard error of the mean (SEM) and were analyzed using the GraphPad Prism 7 software. Statistical analyses of RT-qPCR data and changes in body weight and food intake of Lep^{ob} mice before and after saline or leptin treatment were done by one-way ANOVA followed by Tukey's test. Quantification of CART-ir fiber density was performed in one section and one side of the Arc (n=3/group) at the tuberal level (image 67, Allen Mouse Brain Atlas). Fiber density was quantified by integrated optical density using fixed illumination, background normalization and gray scale in Image J (NIH). Quantification of colocalization between GFP- and Laminin-ir was performed in one section and one side of the PMv (n=4-5, Image 76, Allen Mouse Brain Atlas). F test to compare variances and one-way ANOVA followed by Tukey's test were used. Significance was set at $p< 0.05$.

References

Allison, M.B., Pan, W., MacKenzie, A., Patterson, C., Shah, K., Barnes, T., Cheng, W., Rupp, A., Olson, D.P., and Myers, M.G., Jr. (2018). Defining the Transcriptional Targets of Leptin Reveals a Role for Atf3 in Leptin Action. Diabetes *67*, 1093-1104.

Allison, M.B., Patterson, C.M., Krashes, M.J., Lowell, B.B., Myers, M.G., Jr., and Olson, D.P. (2015). TRAP-seq defines markers for novel populations of hypothalamic and brainstem LepRb neurons. Mol Metab *4*, 299-309.

Burger, L.L., Vanacker, C., Phumsatitpong, C., Wagenmaker, E.R., Wang, L., Olson, D.P., and Moenter, S.M. (2018). Identification of Genes Enriched in GnRH Neurons by Translating Ribosome Affinity Purification and RNAseq in Mice. Endocrinology *159*, 1922-1940.

Fresno, C., and Fernandez, E.A. (2013). RDAVIDWebService: a versatile R interface to DAVID. Bioinformatics *29*, 2810-2811.

Heiman, M., Kulicke, R., Fenster, R.J., Greengard, P., and Heintz, N. (2014). Cell type–specific mRNA purification by translating ribosome affinity purification (TRAP). Nature Protocols *9*, 1282.

Huang da, W., Sherman, B.T., and Lempicki, R.A. (2009a). Bioinformatics enrichment tools: paths toward the comprehensive functional analysis of large gene lists. Nucleic Acids Res *37*, 1-13.

Huang da, W., Sherman, B.T., and Lempicki, R.A. (2009b). Systematic and integrative analysis of large gene lists using DAVID bioinformatics resources. Nat Protoc *4*, 44-57.

Krashes, M.J., Shah, B.P., Madara, J.C., Olson, D.P., Strochlic, D.E., Garfield, A.S., Vong, L., Pei, H., Watabe-Uchida, M., Uchida, N.*, et al.* (2014). An excitatory paraventricular nucleus to AgRP neuron circuit that drives hunger. Nature *507*, 238-242.

Leshan, R.L., Bjornholm, M., Munzberg, H., and Myers, M.G., Jr. (2006). Leptin receptor signaling and action in the central nervous system. Obesity (Silver Spring) *14 Suppl 5*, 208S-212S.

Trapnell, C., Hendrickson, D.G., Sauvageau, M., Goff, L., Rinn, J.L., and Pachter, L. (2013). Differential analysis of gene regulation at transcript resolution with RNA-seq. Nat Biotechnol *31*, 46-53.

Trapnell, C., Roberts, A., Goff, L., Pertea, G., Kim, D., Kelley, D.R., Pimentel, H., Salzberg, S.L., Rinn, J.L., and Pachter, L. (2012). Differential gene and transcript expression analysis of RNA-seq experiments with TopHat and Cufflinks. Nat Protoc *7*, 562-578.